A Photographic Atlas of Rock Breakdown Features in Geomorphic Environments

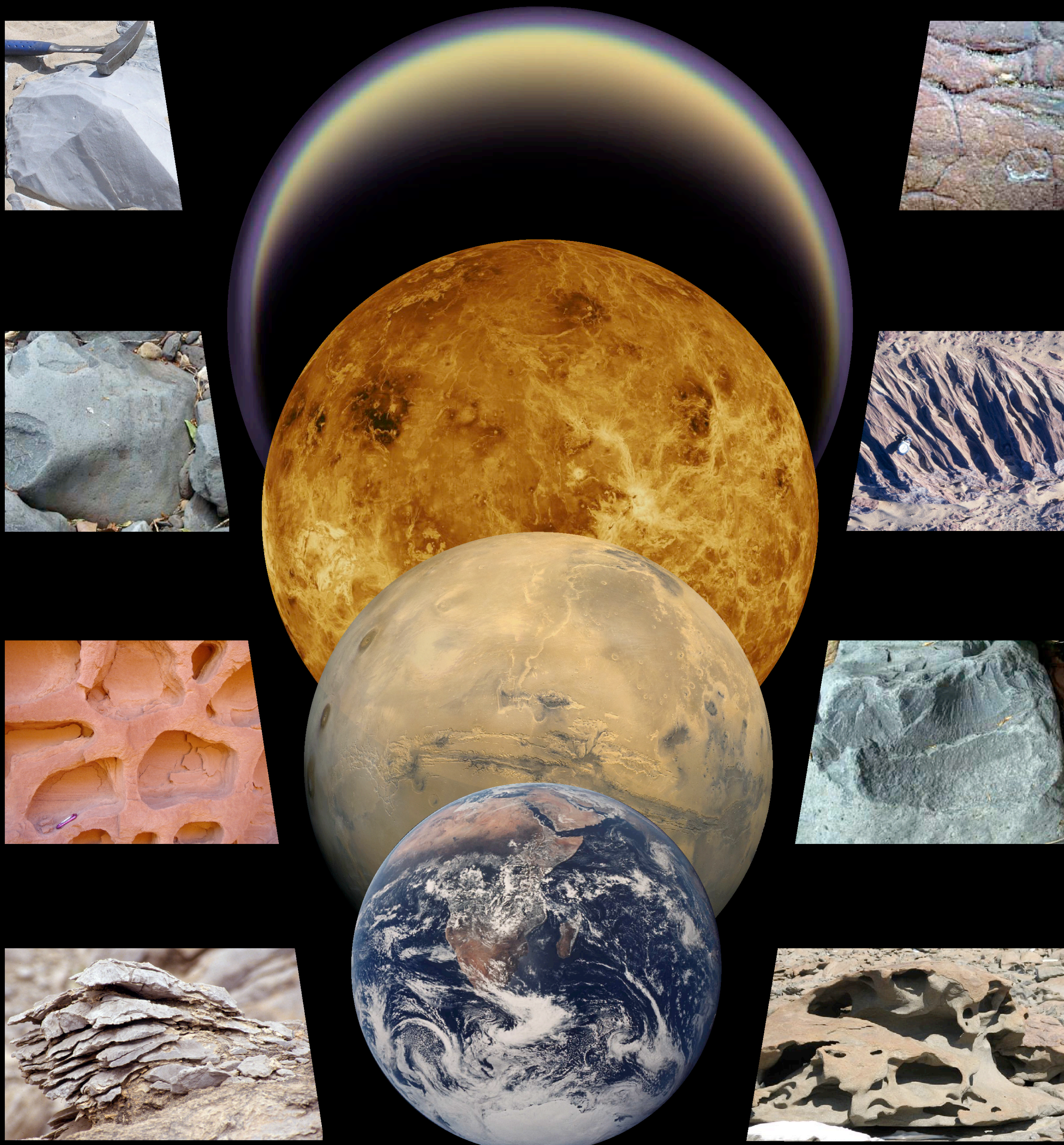

Mary Bourke & Heather Viles (Eds.)

Cover design by Leslie Bleamaster, Planetary Science Institute.
Planetary images include hemispheric views and mosaics from top to bottom:
Titan (PIA07774 NASA/JPL/Space Science Institute, Blue Green Red spectral filters)
Venus - PIA00104 NASA/JPL-Caltech (false color radar mosaic)
Mars - USGS (Viking mosaic)
Earth - Apollo 17 (photograph)
Images courtesy of NASA, the US Geological Survey, JPL-Caltech, and the Space Science Institute - field images taken from contributions herein.

A Photographic Atlas of Rock Breakdown Features in Geomorphic Environments

Mary C. Bourke[1, 2] and Heather A Viles[2] (Eds.)

Contributing Authors:

Dr. Mary C. Bourke[1, 2]
Mr. J. Alexander Brearley[3]
Mr. Randall Haas[4]
Dr. Heather A. Viles[2]

[1]Planetary Science Institute, 1700 E Ft. Lowell, Tucson, Arizona, 85719 USA.
[2]Oxford University Center for the Environment, University of Oxford, Oxford, OX13QY, UK.
[3]Department of Geography, University of Reading, Reading, UK.
[4]Western Mapping Company, Tucson, Arizona 85719-2360.

International Association of Geomorphologists
Working Group on Planetary Geomorphology

First published in 2007
By the Planetary Science Institute,
1700 E. Fort Lowell, #106,
Tucson,
Arizona 85719,
USA.

Digital Copy available online ISBN 0-9785236-0-1

Acknowledgements:

The following reviewers made valuable suggestions that improved the content of this atlas:

Dr. Kathryn Amos, University of New South Wales, Canberra, Australia.
Dr. Nathan Bridges, Jet Propulsion Laboratory, California, USA.
Prof. Paul Carling, University of Southampton, United Kingdom.
Dr. Jon Clarke, Geoscience Australia, Canberra, Australia.
Dr. Jennifer Grier, Planetary Science Institute, Arizona, USA.
Dr. Julie Laity, California State University, California, USA.
Dr. Piotr Migoń, University of Wroclaw, Poland.
Dr. Nichole Richmond, Planetary Science Institute, Arizona, USA.

In addition to our own collection, we are very grateful to the following for contributing images to this atlas.

Dr. Mircea Badescu, Jet Propulsion Laboratory, California, USA.
Dr. Nathan Bridges, Jet Propulsion Laboratory, California, USA.
Ms. Julia Fonseca (M.Sc.), Tucson, Arizona, USA.
Prof. Andrew Goudie, St Cross College, University of Oxford, UK.
Dr. Julie Laity, California State University, California, USA.
Mr. Carl Matter, Tucson, Arizona, USA.
Dr. Gordon Osinski, Canadian Space Agency, Canada.
Dr. Keith Richardson, University of Lancaster, United Kingdom.
Dr. Stewart Sherrit, Jet Propulsion Laboratory, California, USA.

The compilation of this atlas was funded, in part, by a grant from NASA's Planetary Geology and Geophysics Program.

Table of Contents

Chapter 1: Introduction

Bourke, M.C. and Viles, H.A.

A primary goal of geomorphological enquiry is to make genetic associations between process and form. In rock breakdown studies, the links between process, inheritance and lithology are not well constrained. In particular, there is a need to establish an understanding of feature *persistence*. That is, to determine the extent to which *in situ* rock breakdown (*e.g.,* aeolian abrasion or salt weathering) masks signatures of earlier geomorphic transport processes (*e.g.,* fluvial transport or crater ejecta). Equally important is the extent to which breakdown during geomorphic transport masks the imprint of past weathering (Viles *et al.*, 2005).

Sedimentary particles may retain their primary form to a substantial and recognizable degree after more than one cycle of transport (Allen, 1985). This is due to the predetermination of shape by factors such as the deposition of crystal boundaries (*e.g.,* grains released from igneous and metamorphic rocks) and the attitude and spacing in the rock of planar fractures including bedding, joints and cleavage. The exception to this is where there has been breakage (Allen, 1985) as is found in fluvial, ejecta and talus environments. Often this initial form is overprinted to some degree during transport (*e.g.,* fluvial, glacial) and/or by subsequent alteration by erosion or weathering. These specific geomorphic processes on Earth can be shown to produce a particular size and shape of morphological response on rocks. For example, rocks subject to fluvial transport tend to be well rounded (Howard, 1998), whilst those freshly collapsed from bedrock walls are angular. However, the situation is complicated by lithology and some rocks respond more rapidly and in different styles to breakdown processes. Over time, the inheritance of both initial lithology and past processes may complicate the relationship between current process and morphological response.

Similar landforms and features can result from quite different sets of processes and histories (see discussion in Beven, 1996). Equifinality is of particular concern when conducting geomorphological enquiry on other planetary bodies using only remotely sensed data. By way of example, pits observed on the surface of clasts can be formed by grinding, micro-impact, structural controls such as vesicles in basalt, or selective mineral loss. In addition, flutes and grooves are known to form by both aeolian and fluvial processes.

On Earth we generally have the ability to visit a field area and place a sample rock in its geomorphic context by mapping the surrounding landforms and sediments. This is more difficult on planets and moons such as Mars, Venus and Titan. Data from Landers and Rovers return high resolution images that indicate a range of boulder morphologies and surface features (Fig. I1) (see also Bridges *et al.*, 1999; Greeley *et al.*, 2004; Thomas *et al.*, 2005). Often the resolution is high enough to permit the observation and analysis of individual facet-scale features, in addition to the traditional observations of clast roundness and sphericity. These data are often used to interpret the transport and environmental history of the rock. For example, studies of rock morphology, placement and bedforms at the Mars Pathfinder landing site suggested that the sediments were the typical deposits of catastrophic floods. However, definitive fluvial signatures were difficult to identify on the rocks (*e.g.*, Golombek *et al.*, 1999). This is likely due to the fact that they have been subject to sub-aerial erosion for more than two billion years.

The use of rock features in this way raises the important question: Can features on the surface of a rock reliably indicate its geomorphic history? This has not been determined for rock surfaces on Earth or other planets. A first step towards constraining the links between process, inheritance, and morphology is to identify *pristine* features produced by different process regimes. The purpose of this atlas is to provide a comprehensive image collection of breakdown features commonly observed on boulders in different geomorphic environments. The atlas is intended as a tool for planetary geoscientists and their students to assist in identifying features found on rocks on planetary surfaces.

In compiling this atlas, we have attempted to include features that have formed 'recently' and where the potential for modification by another geomorphic process is low. However, we acknowledge that this is, in fact, difficult to achieve when selecting rocks in their natural environment. We group breakdown features according to their formative environment and process (Fig.I2).

In selecting images for inclusion in the atlas we were mindful to cover a wide range of climatic zones. For example, in the weathering chapter, clast features are shown from locations such as the hyper-arid polar desert of Antarctica and the semi-arid canyons of central Australia. This is important as some features (*e.g.,* alveoli) occur across climate regimes. We have drawn on the published geomorphological literature and our own field experience. We use, where possible, images of extrusive igneous rocks as the data returned from Mars, Venus and the Moon indicates that this is the predominant rock type.

One of the purposes of this atlas is to expand the range of surface features that are known to indicate a particular geomorphic environment or process history. The surface features on boulders in some environments such as aeolian and weathering are well understood. In contrast, those in fluvial or ejecta environments are not. Therefore we have presented a comprehensive assemblage of features that are likely to be produced in each of the geomorphic environments. We hope that this atlas will trigger more research on diagnostic features, particularly their morphometry and detailed morphology, their persistence and rates of formation. In this first edition of the atlas we detail the features found on clasts in three geomorphic environments: aeolian, fluvial and weathering. Future editions of the atlas will include chapters on ejecta, micro-impacts, coastal, colluvial, glacial and structural features.

Figure I1 Images of rocks on the surface of other planets and moons in our solar system
a) The surface of Mars taken by the US Viking Lander 2 in 1976 (Image 21A024-BB3)

b) ‘Big Joe’ on the surface of Mars taken by the US Viking Lander 1 in 1977 (Image 11D066-BB4).

c) The surface of Mars taken by the US Viking Lander 1 in 1977 (Image 12D039-BB2)

d) & e) One of the few images from the surface of Venus. Image taken by the Russian probes Venera 13 and 14, in 1982. Venera 14 sampled the soil where it landed, and found a type of basalt also common on Earth (Image credit: NASA)

f) One of the few images taken by the European Huygens Probe of the surface of Titan (2005). In view are cm-scale pebbles. A current popular hypothesis is that they are composed of water ice, and lie on a darker, finer-grained substrate.

g) Image of Rock “Moe” from the pathfinder site on Mars (1997) (Image PIA01565)

h) Image of Rock “Half-dome” from the pathfinder site on Mars (1997)

i) Pancam image of "FuYi” rock taken by Spirit Rover (2006) along the edge of an arc-shaped lava feature called "Lorre Ridge"

j) Microscopic Imager on the Opportunity Rover image of “Roosevelt”. The image shows detailed structure of an outcrop located at the edge of Erebus Crater.

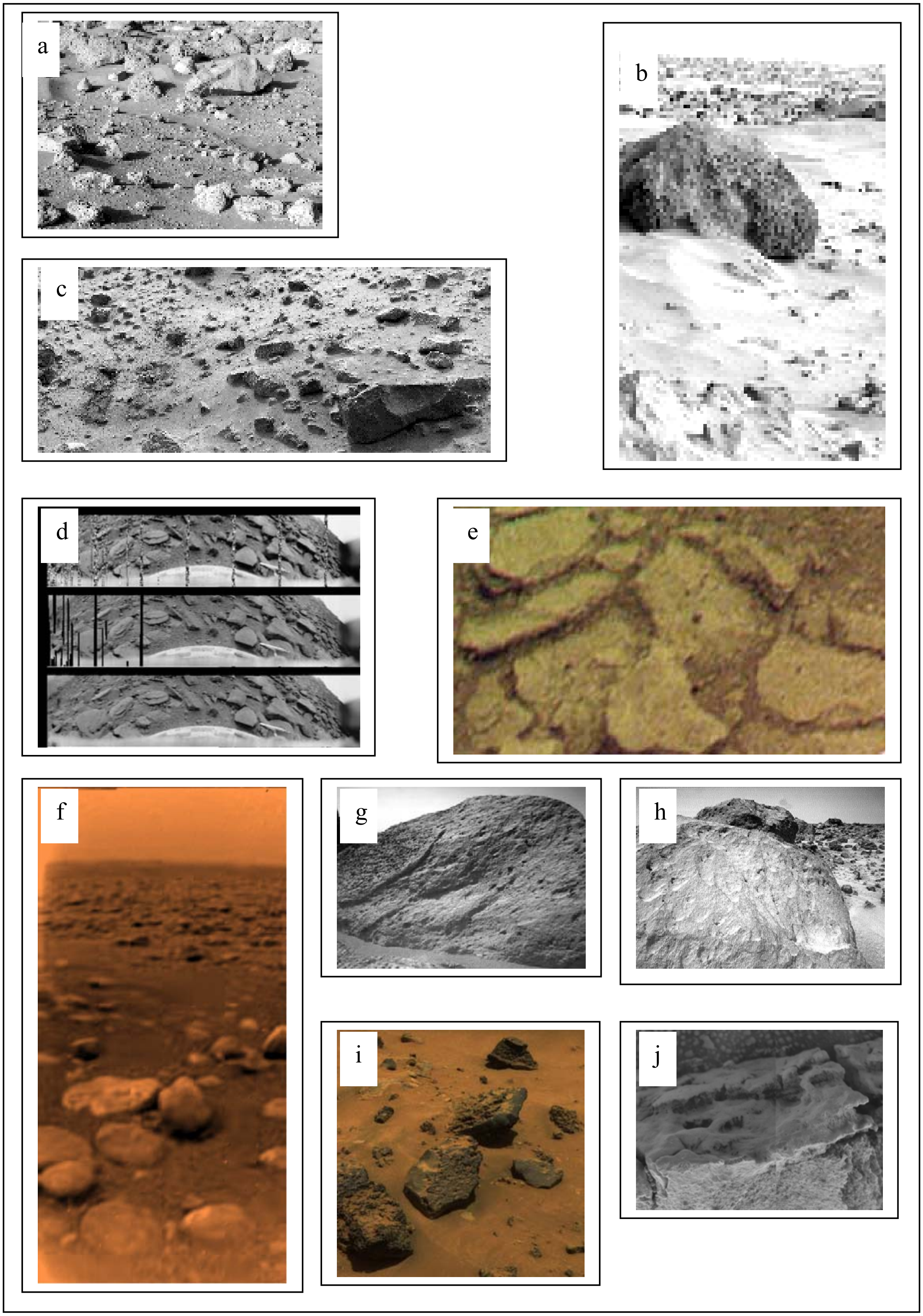
a
b
c
d
e
f
g
h
i
j

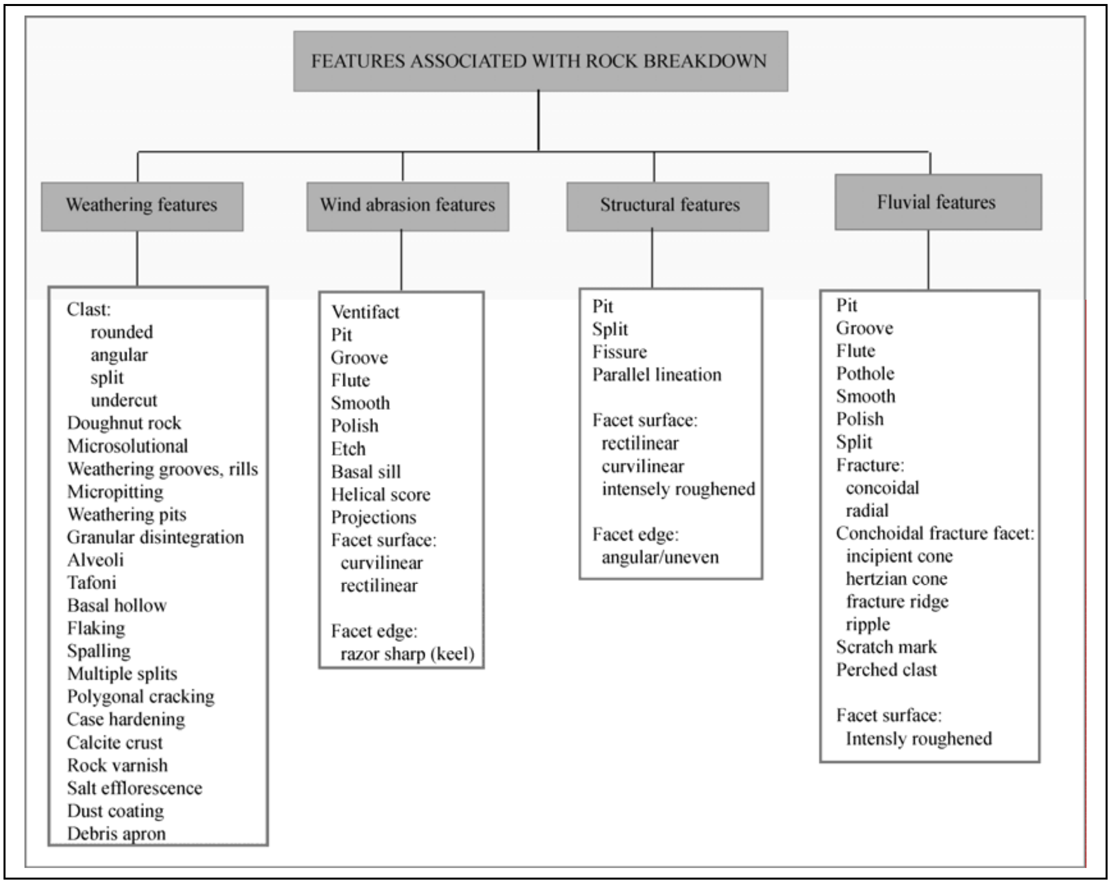

Figure I2 Genetic classification used in the development of the rock breakdown atlas. This will be extended in future editions to include ejecta and micro-impacts.

Chapter 2: Aeolian Features

Viles, H.A. and Bourke, M.C.

Ventifacts in southern Death Valley. Image courtesy of J. Laity.

Introduction

Wind action causes the erosion of boulders through abrasion by entrained particulates. Ever since the pioneering work of, amongst others, W. T. L. Travers in 1870 (as noted in King, 1936) a whole suite of erosional features have been recorded and studied in areas where wind and abrading agents are in ample supply. Much of the early research focused on cataloguing sites in very different parts of the world where wind abrasion features were found (*e.g.*, Bosworth, 1910; King, 1936; Powers, 1936; Wentworth and Dickey, 1935) as well as understanding their formation (*e.g.*, Kuenen, 1928). For palaeoenvironmental research, such features have been used to confirm the past efficacy of wind action, and also to infer dominant wind direction(s) at the time of feature formation (Schlyter, 1995; Sharp, 1949).

Wind abrasion of boulders has been noted on several lithologies in a wide range of environments including deserts, periglacial and coastal settings and has been reported on Mars (see Bridges *et al.*, 1999). There has been much debate over the types of particulates which can cause such abrasion, with most scientists placing major emphasis on sand, whilst some authors suggest that silt and snow can also be effective (Frich, 1988; Schlyter, 1994). See Breed *et al.* (pg. 445-453, 1997) for discussion. In most cases, wind abrasion by particulates has been observed to be concentrated on the upwind side of boulders and outcrops, with the leeside commonly weathered and free from abrasion. Recent estimates from boulders within a coastal structure in Oregon, USA indicate that wind abrasion can proceed at rates of between 0.24 and 1.63 mm a^{-1} (Knight and Burningham, 2003), although very different rates may be found in other localities.

Some previous authors have produced useful guides to the features produced by aeolian action on rocks, including the classic review of Maxson (1940) and the more recent compendium of Laity (1995). Both of these contain images which complement this atlas.

<u>Ventifact</u>

Scale: cm to m

Feature description:
Ventifacts may be simply defined as rocks shaped by aeolian abrasion (Cooke *et al*., 1993). The term was introduced by Evans (1911) to describe wind-faceted stones, the surfaces of which are flattened such that they intersect at sharp angles (Goudie, 2004b). Such ventifacts have clear wind sculpted facets which themselves often have a whole suite of smaller abrasion features developed on them. A common shape for small faceted ventifacts is a streamlined, almond or brazil nut shape dominated by two or three surface facets.

Figure A1 A three-faceted ventifact (often called 'dreikanter') from the Cunene River terrace, Namibia. Image courtesy of M. Bourke.

Figure A2 A dolerite ventifact in the Namib Desert, Africa. Image courtesy of H. Viles.

Sharp facet edge (keel)

Scale: several mm to cm long (depending on size of facet), and < 1 mm wide

Feature description:
Facets are thought to be abraded at right angles to the formative wind where sand is the dominant agent of abrasion. The edge between facets is often razor sharp, where each facet is being actively abraded and/or where the rock is fine-grained. Facet edges are also often called keels (*e.g.*, Knight, 2005), and can be linear or serrated (Knight and Burningham, 2001). The keel is usually aligned perpendicular to the prevailing wind direction and thus can be used on fossil forms to infer palaeo-wind direction. However, recently Knight (2005) drew attention to the need to take care with such inferences because of the role, in some circumstances, of more localized controls on keel orientation (such as boulder shape and local wind flow complexity).

Figure A3 Faceted carbonate rock, Little Cowhole Mountains (Mojave Desert), California. Image courtesy of N. Bridges.

Figure A4 A sharp facet edge on ventifact from the Cunene River terrace gravel Namibia. Note also the polished sheen. See figure A1 for scale. Image courtesy of C. Matter. See also Figure A11.

Straight facets

Scale: cm

Feature description:
Smaller facets carved into ventifacts by aeolian abrasion are generally straight in profile (*i.e*. they have a flat face), although their shape can be affected by the pre-existing clast form. Smaller rocks are also thought to produce simpler facets (*i.e.* planar and smooth faces), than larger ones where pitting, fluting and other features are likely to develop (Laity, 1994).

Figure A5 A straight facet on ventifact from the Cunene River terrace gravel Namibia. See figure A1 for scale. Image courtesy of C. Matter.

Curvilinear facets

Scale: cm to m

Feature description:
Larger facets are usually abraded into slightly curved forms (Cooke *et al.*, 1993). Indeed, large ventifacts abraded by sand often have a highly convex windward facet with the top part receding more rapidly than the lower section. Over time, long-term and intense abrasion may eventually produce semi-planar surfaces (*e.g.*, Laity, 1995, Fig.12).

Figure A6 Faceted carbonate rock, Little Cowhole Mountains (Mojave Desert), California. Image courtesy of N. Bridges.

Flutes

Scale: mm to cm

Feature description:
Flutes are near-linear depressions with U-shaped cross-sections, which are closed at the upwind end. They are thought to form on low angled or horizontal surfaces, and they have been observed to get shorter and deeper as the surface inclination increases. Lancaster (1984) noted that, in the Namib Desert, there was some lithological control of flute size – with coarse-grained rocks possessing larger and deeper flutes than fine-grained rocks. According to Cooke *et al.* (1993) flutes and grooves are said to develop in the early stages of ventifaction, usually originating from pits and becoming shallower downwind. They are also said to be better developed on large rather than small rocks. Breed *et al.* (1997) note the presence of y-shaped junctions in fields of flutes, where the junctions close in the downwind direction. Flutes have been recorded having widths and depths ranging from a few mm to several cm. Flute formation is still debated, but the general consensus is that flutes are formed parallel to the wind on the windward side of ventifacts as a result of abrasion by sand. Experimental studies by Whitney (1979) suggested that fluting on leeward sides could be created by dust entrained in vortical flow within winds. However the efficacy of dust as an abrading agent is the subject of debate (see Breed *et al.*, 1997). Flutes can also be formed by fluvial abrasion (see Figs. F24-F26).

Figure A7 Aeolian flutes, and grooves, Dahkla Oasis, Egypt. Image courtesy of A. Goudie. The watch used for scale is ~4 cm in diameter.

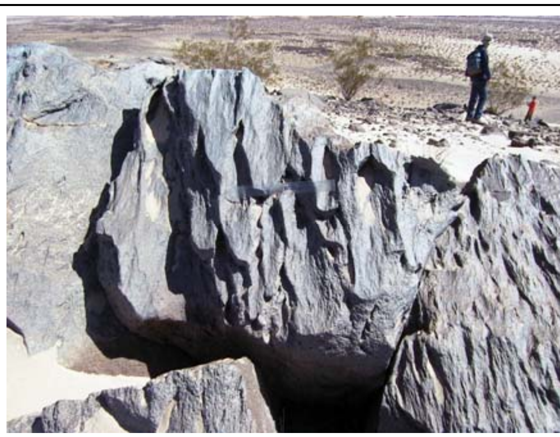

Figure A8 Aeolian flutes, Cady Mountains, California. Transparent ruler, with blue lettering, is on rock for scale. Image courtesy of J. Laity.

Flutes (cont.)

Figure A9 Aeolian flutes associated with stretched vesicles in Basalt, Cady Mountains, California. Image courtesy of J. Laity**.**

Figure A10 Aeolian flutes on a basalt rock Cady Mountains, California. Image courtesy of J. Laity.

Figure A11 Aeolian flutes on carbonate rock, Cowhole Mountains, California. Note sharp, serrated keel perpendicular to wind flow and the presence of flutes on either side reflecting bi-directional wind regime. Image courtesy of J. Laity**.**

Grooves

Scale: mm to cm

Feature description:
Grooves are similar features to flutes, and many workers group them together. However, Laity (1994), amongst others, defines grooves as being longer than flutes and open at both ends. They form on gently inclined surfaces, are often separated by sharp-crested, sometimes sinuous ridges, and their scale varies from mm to cm. Laity (1995) measured groove widths up to 7 cm in the Little Cowhole Mountains. Grooves can also be formed by fluvial abrasion (Richardson and Carling, 2005).

Figure A12 Aeolian grooves developed on chalk, Farafra Oasis, Egypt. Note geological hammer for scale. Image courtesy of A. Goudie.

Figure A13 Aeolian grooves (white arrow) developed on marble, central Namib Desert, Africa. The marble outcrop is about 50 cm wide. Image courtesy of H. Viles.

Grooves (cont.)

Figure A14 Aeolian grooves (and flutes) on basalt rock Cady Mountains, California. Image courtesy of J. Laity**.**

Etching

Scale: mm to cm

Feature description:
Lancaster (1984) describes how abrasion by dust (and sand) can produce etching, whereby lithological and mineralogical variations in the rock are accentuated. Thus, less resistant minerals or bands within a facet will become preferentially attacked, forming sometimes complex etching patterns. For example, abrasion can pick out foliation structures producing flute-like features, whether or not the foliation is parallel to the wind direction. Laity (1994) notes that, unlike flutes and grooves, aeolian etching patterns can be irregular.

Figure A15 Etched sandstone boulder, Meteor Crater, Arizona. Note the overprinting of etching on alveoli weathering. Image courtesy of M. Bourke.

Figure A16 Etched carbonate rock, Little Cowhole Mountains (Mojave Desert), California. Image courtesy of N. Bridges.

Figure A17 Etched rock, Lake Vida, Dry Valleys, Antarctica. Full separation may have been enhanced by freeze-thaw action. Image courtesy of M. Badescu and S. Sherrit.

Pits

Scale: mm to cm

Feature description:

Pits (also called re-entrants and salients by Cooke *et al.*, 1993) appear to result from abrasion attacking pre-existing heterogeneities in the rock surfaces, such as cracks, less resistant mineral grains, or vesicles. Pits are defined by Laity (1994) as closed depressions, often of irregular shape. According to Greeley and Iverson (1985) pits form most commonly on windward facets inclined at between 55^o and 90^o to the wind. However, at the SEM scale Whitney (1979) identifies *vortex pits* as being produced by dust impacts within vortices affecting leeward facets, but such pits have not been recorded at the visible scale. Vortex pits appear to differ from sand-abraded pits because of the presence in the former of fine-textured dendritic abrasion within the pits (see Breed *et al.*, 1997, Fig. 446). Pits may also be oriented at an angle to the surface on which they are developed. Christiansen (2004) notes elongated pits on Antarctic rock surfaces which form parallel to wind direction as a transitional feature between pits and grooves.

Figure A18 Pits in basalt, Cady Mountains, California. Image courtesy of J. Laity.

Helical scores

Scale: mm to cm

Feature description:
Relatively uncommon features, helical scores are corkscrew shaped depressions which deepen and spiral in a downwind direction, terminating in a sharp point. They have been recorded, for example, on marble in the Mojave Desert, California (Laity, 1995). Their genesis is uncertain, but they are thought to evolve from grooves or flutes and be produced under very high wind velocities. Similar forms (compound parallel-sided furrows) are also noted in fluvial systems (Richardson and Carling, 2005).

Figure A19 Helical scores developed on marble in central Namib Desert. Image courtesy of H. Viles.

Figure A20 Helical scores developed on carbonate rock, Little Cowhole Mountains, California. Image courtesy of J. Laity.

Projections (fingers, knobs and ridges)

Scale: mm to cm

Feature description:
Projecting fingers are observed on very abraded facets, where small patches of highly resistant minerals have withstood abrasion in comparison with the surrounding surface. In some cases a visible inclusion can be seen at the top of the knob or finger, which has protected the underlying surface from erosion. Alternative names for these features include 'collar studs' (Powers, 1936) and 'dedos' (McCauley *et al.*, 1979). Highly resistant mineral veins within rocks may also withstand abrasion to produce projecting ridges.

Figure A21 A finger projection (towards viewer, white arrow) on Hermansberg Sandstone, Finke River Gorge, Australia. Image courtesy of M. Bourke.

Figure A22 Differentially eroded ridges (quartz veins) in a basalt rock, Cady Mountains, California. Image courtesy of N. Bridges.

Smoothing and polishing

Scale: mm to m

Feature description:
Smoothing and polishing of facets is one of the most commonly observed features associated with wind abrasion. Polish can occur across whole facets and also within flutes and grooves. The degree of polishing is a good indication of the relative age of the ventifact although rates vary with lithology (Laity, 1995). Wind polishing can produce glassy surfaces on suitable lithologies (Christiansen, 2004). Smoothing and polishing can also result from fluvial abrasion (see Fig. F5).

Figure A23 A polished ventifact surface from the Hartman Valley, northern Namibia. Image courtesy of M. Bourke.

Figure A24 A polished ventifact from the Little Cowhole Mountains, California. Image courtesy of Julia Fonseca.

Figure A25 Polished facet on ventifact, Lake Vida, Dry Valleys, Antarctica. Image courtesy of M. Badescu and S. Sherrit.

Basal sill

Scale: cm

Feature description:
Towards the base of larger ventifacts and rocks there is often a zone with minimal abrasion features developed, where soil or debris has protected the rock from abrasion. This produces a step or sill-like feature at the base of a facet. These sills can also form in aggressive weathering environments (see Fig. W19).

Figure A26 Arrow indicates basal sill development on a faceted carbonate rock, Little Cowhole Mountains (Mojave Desert), California. Image courtesy of N. Bridges.

Summary table of aeolian features

<table>
<tr><th>SCALE</th><th>TYPE</th><th>NAME</th></tr>
<tr><td rowspan="4">CLAST</td><td rowspan="4"></td><td>VENTIFACT</td></tr>
<tr><td>SHARP FACET EDGE (KEEL)</td></tr>
<tr><td>STRAIGHT FACET</td></tr>
<tr><td>CURVILINEAR FACET</td></tr>
<tr><td rowspan="8">FACET</td><td rowspan="6">MATERIAL LOSS</td><td>FLUTES</td></tr>
<tr><td>GROOVES</td></tr>
<tr><td>ETCHING</td></tr>
<tr><td>PITS</td></tr>
<tr><td>HELICAL SCORES OR FORMS</td></tr>
<tr><td>PROJECTING FINGERS, KNOBS AND RIDGES</td></tr>
<tr><td rowspan="2">NO MATERIAL LOSS OR GAIN</td><td>SMOOTHING AND POLISHING</td></tr>
<tr><td>BASAL SILL</td></tr>
</table>

Chapter 3: Fluvial Features

Bourke, M.C., Haas, W.R., Brearley, J.A., and Viles, H.A.

View looking downstream along Oak Creek Canyon, Arizona. Image courtesy of M. Bourke.

Introduction

In this chapter, we describe morphological features that are present on fluvial clasts. The features are typical of rivers from all flow and climatic regions. Sedimentary facies that contain such clasts include floodplains, terraces, channel beds, channel bars and alluvial fans. The clasts of interest in this atlas are cobble size and larger (*i.e.* >6.4 cm intermediate axis).

Cobbles, along with other sediment sizes, usually enter the fluvial system through lower order tributaries or can be eroded from adjacent (often, but not always, alluvial) sediments. In steep upstream reaches or areas of bedrock confinement, clasts may be delivered directly from canyon walls (*e.g.,* by toppling, avalanche or landslide Howard, 1998) or by block quarrying (plucking) from in-channel bedrock exposures (Tinkler and Wohl, 1998). Boulders and megaclasts (> 4.1 m, Blair and McPherson, 1999) are sometimes introduced in this way. They may also be the remnant load of a palaeo- higher magnitude, flow regime *(e.g.,* glacial outwash). In many rivers on Earth these large boulders and megaclasts are now 'non-transported', that is, they are stable relative to the surrounding bedload under the current flow regime (Richardson and Carling, 2005). Megaclasts that are positioned within the channel develop a myriad of features that are similar to bedrock bedforms (Richardson and Carling, 2005). Canyon wall collapse or impact by clasts during high magnitude floods may introduce smaller fragments of fluvially sculpted bedrock into the channel. In this way, clasts with erosional features that were formed on a relatively stable bedrock surface may be incorporated into the channel as bedload. Although we include some of these features in this atlas (*i.e.*, potholes and flutes), a recent review of bedrock channel forms by Richardson and Carling (2005) has identified approximately 140 features, all of which could potentially exist on introduced clasts. Readers are encouraged to consult that publication for further detail.

The mobilization of fluvial sediments often alters the surface morphology of clasts, and this chapter is primarily concerned with these features. Fluvial sediment is transported in three ways: wash, suspension and traction (Richards, 1982). Cobbles and larger size clasts generally tend to be transported as traction load. However, if the flow magnitude is sufficiently strong, they may be transported in suspension (*e.g.*, Ritter, 1975). Traction load is generally moved by dragging and saltation. Transport of clasts in this way subjects them to percussion, grinding and abrasion, causing clasts to split, fracture and become polished (Kuenen, 1956; Marshall, 1927).

Previous investigators have cited rounding (Howard, 1998), polishing, smoothing, fracturing and fissuring (Marshall, 1927) as indirect evidence of fluvial transport. In addition to these we have identified another thirteen signatures of fluvial transport. Eight of the additional features are related to percussion events. Such features include: percussion-fracture facet, percussion-fracture ridges (distal and proximal), bulb of percussion, radial fissure, undulation, hertzian cone, incipient cone, and termination. Pits, although related to percussion events, are not related to percussion fracture generation and are discussed separately. The remaining features, striations and scratches, potholes, and flutes, are primarily related to abrasion events. Many of the features described in this chapter are not, of themselves, diagnostic of a fluvial environment. For example, percussion fracture features are also found on ejecta and colluvial clasts that have been subjected to percussion.

Percussion Terminology

The term 'percussion fracture' requires explanation. For the purpose of this atlas, percussion impact refers to any collision between a clast and another clast or bedrock. If a certain set of conditions are met during a percussion event, a percussion fracture may result. Cotterell and Kamminga (1987) identify three types of percussion fractures: conchoidal, bending, and wedging. Of these, conchoidal fractures appear to be the most relevant when considering geological processes.

Geological literature, to our knowledge, does not provide a terminology for describing conchoidal fracturing. Archaeologists, on the other hand, have devoted considerable effort to understanding such fractures (Andrefsky, 1994; Whittaker, 1994) because the technology permitted hominids, for over 2.5 million years, to systematically reduce stone into tools with sharp cutting edges (Fig. F1). As the principles of physics that govern percussion flaking are the same whether a human action, flood event, or gravity causes two rocks to collide, many of the terms used herein are borrowed or adapted from archaeological literature.

Conchoidal fractures are a special case of percussion fracture in which a cone-shaped stress wave passes through a rock resulting in the detachment of a *flake* from a *core* (Fig. F2). In rare instances, the detached flake will take the form of a cone known as a hertzian cone. But, conchoidal fractures do not always completely propagate, creating crescentic surface depressions known as incipient cones or ring cracks. If a conchoidal fracture fully propagates on the margin of a clast, a partial hertzian cone is formed and a flake is detached from the core (Fig. F2). The conchoidal fracture manifests on the core as a concave facet and on the flake as a convex facet.

Conchoidal fracture faces are associated with a host of related sub-features. These sub features present important diagnostic criteria for identifying and analyzing percussion events. When considered in combination with other clast features, conchoidal fracture features can provide evidence of percussion that may indicate fluvial transport processes. A limited number of formal and informal archaeological experiments and ethnographic observations have shed light on the complex set of variables that influence clast fractures (Cotterell and Kamminga, 1987; Dibble and Whittaker, 1981; Speth, 1972; Speth, 1974; Speth, 1975; Speth, 1981).

The current state of knowledge allows for a few concrete statements about the relationships between percussion fracture variables. First, all else being equal, lithology will affect the nature of the fracture. Rocks such as chert, flint, rhyolite and basalt are relatively brittle, elastic and homogenous, and are more likely to propagate a percussion fracture. Coarser, less homogeneous rocks such as granite are less conducive to conchoidal fracturing at the clast scale. Given a particular mineralogy, the next most important factor affecting flake morphology is collision and core geometry. Conchoidal fractures most-often occur on the acute edges of clasts at an acute striking angle relative to the striking platform (Fig. F3). In general, the closer the platform angle is to 90°, the greater the flake length (Speth, 1981). Platform angles greater than 90° deter the propagation of percussion fractures. Finally, and perhaps most intuitively, striking force plays a key role in the morphology of percussion fractures (Dibble and Whittaker, 1981; Speth, 1972; Speth, 1974). Given a particular mineralogy and collision geometry, greater striking forces will produce larger percussion fractures. These three simple relationships between flake morphology and mineralogy, geometry, and force are fundamental to understanding how percussion fractures occur on clasts.

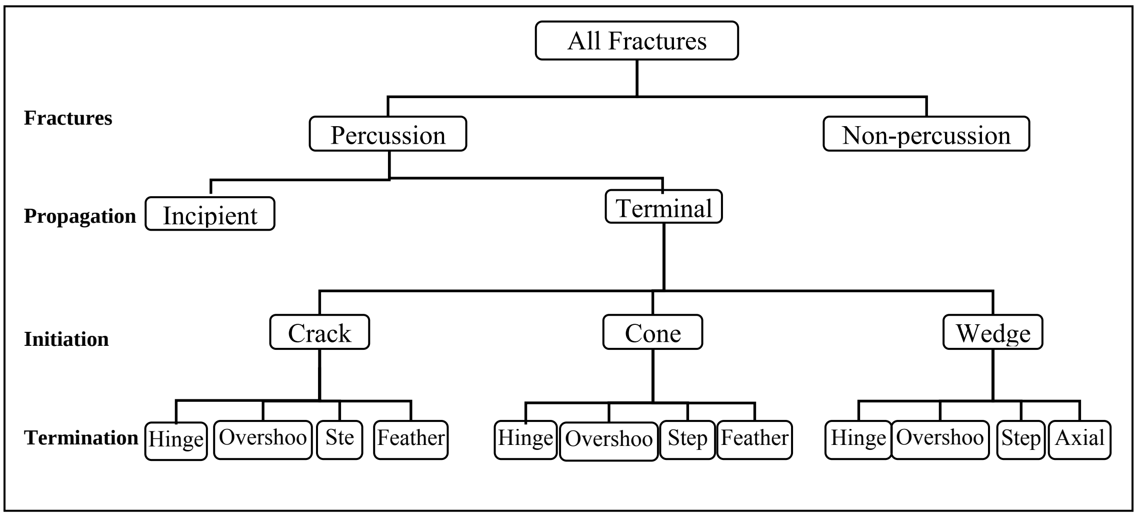

Figure F1 Classification scheme for percussion fractures (Cotterell and Kamminga, 1987).

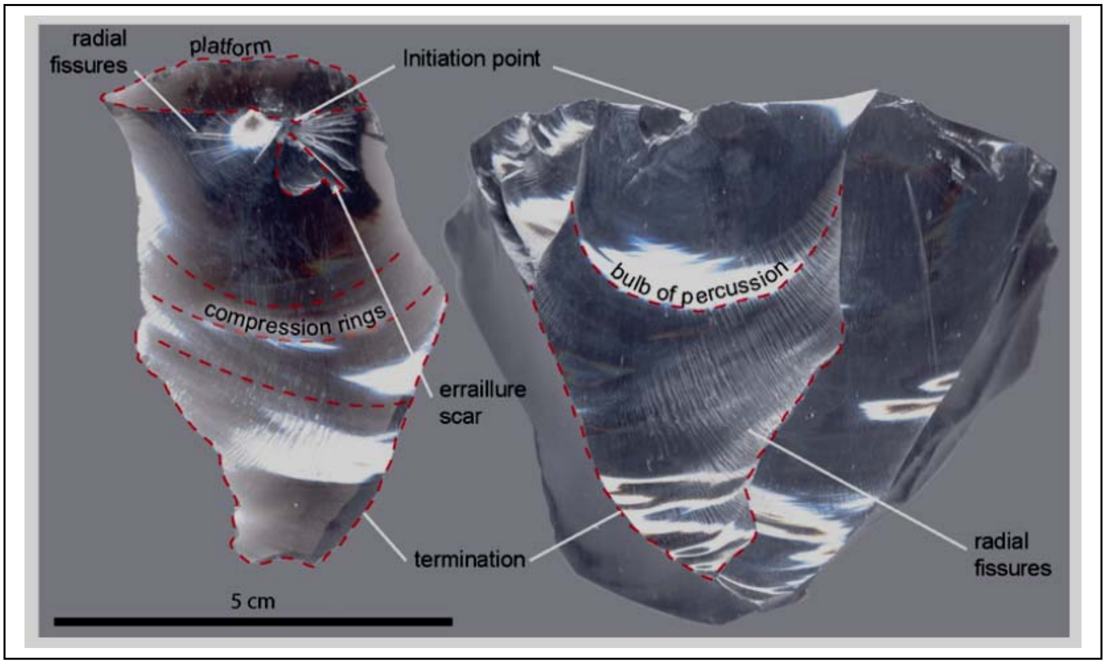

Figure F2 Diagnostic percussion-fracture features on volcanic glass from Glass Buttes, Oregon. The flake on the left was detached from the core on the right (percussed and imaged by R. Haas).

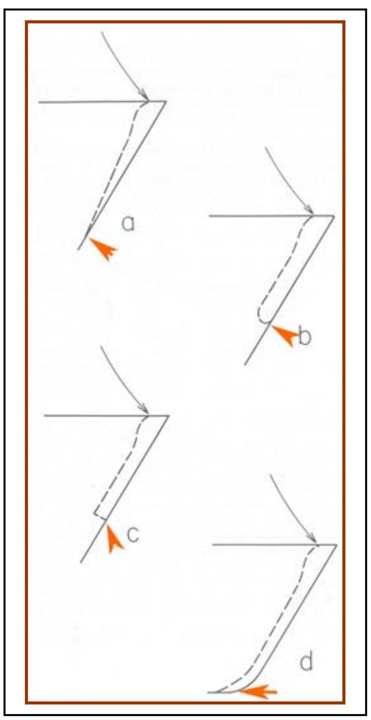

Figure F3 Termination classification used in this study after Cotterell and Kamminga (1987). Grey arrow indicates direction of impact and dashed line shows pathway of fracture. Orange arrow indicates termination location. There are three types of terminations viewed in profile:

1. Straight (also known as feather, (a)).
2. Outcurved terminations curve away from the mass of the clast and can be one of two types: hinge (b) or step (c).
3. Incurved (also known as overshoot (d)). See section on terminations for further discussion. Figure after Whittaker (1994).

Rounding

Scale: clast

Feature description:
Clast roundness is perhaps the most cited indicator of fluvial transport. Abrasion (also known as corrasion) involves the mechanical erosion of rocks by numerous impacts from other sediment particles transported in the fluid. These particles may be carried in suspension or as bedload, or both. Each impact, if sufficiently energetic, breaks off a small piece of the surface. This may be at the scale of a small part of a grain (in the case of suspended load), or as much as a substantial chip of rock in the case of coarse bedload (Richardson and Carling, 2005). Factors that influence roundness are the particle form and the concentration and characteristics of other particles in transport. In fluvial systems, sand acts as an abrasive agent when transported with gravel particles, causing them to round quickly. Roundness increases with transport distance and particle size and decrease with hardness (Allen, 1985).

Figure F4 Rounded and sub-rounded fluvial gravel on channel bed of semi-arid Finke River, central Australia. See also Figure F5 for rounded cobble. Image courtesy of M. Bourke.

Polishing and smoothing

Scale: clast and facet

Feature description:
Suspended sediment can abrade clasts to form extremely smooth, shiny and sometimes gently undulating surfaces (Baker and Kale, 1998; Baker and Pickup, 1987; Hancock *et al.*, 1998; Wohl and Ikeda, 1998). Although individual clasts can be polished, this phenomenon is more often observed on large non-transported clasts and introduced bedrock clasts which were already polished. It is found on hard, dense medium and fine grained textured clasts (*e.g.*, medium sandstone and finer) (Richardson and Carling, 2005).

Figure F5 Polished quartzite cobble sitting on sand on a Cunene River terrace, northern Namibia. Surface markings are incipient cones. Image courtesy of M. Bourke.

Fissure

Scale: clast and facet

Feature description:
The presence of fissures, where cracks can be seen on the rock surface, but without complete detachment, is common in fluvial environments. Fissures can form from multiple causes (*e.g.,* weathering, ballistic impact, rock structure etc.) and are found in many geomorphic environments (fluvial, ejecta, talus slopes etc.). In fluvial environments, fissures result from impact with other transported clasts or by impact against immobile clasts or bedrock. These ballistic forces may also exploit pre-existing structural fissures.

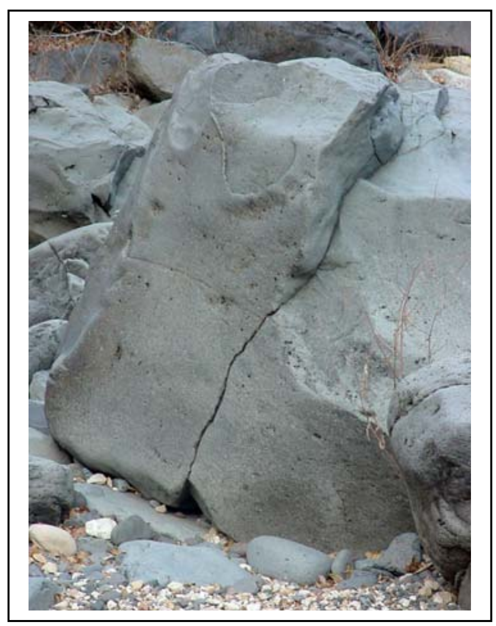

Figure F6 a & b Flood transported clasts in Oak Creek Canyon, Arizona. Large fissure bisects boulder. Note pits evident, most likely vesicles. Image courtesy of M. Bourke.

Broken and split clasts

Scale: clast and facet

Feature description:
In fluvial systems, clasts can be broken into more angular shapes as a result of crushing between larger stones, and impact. For megaclasts (> 4.1 m, Blair and McPherson, 1999) and boulders that are transported infrequently, this is often the primary mechanism of physical breakdown. The resultant clast shape often has a sub-rounded to well-rounded facet that appears truncated by an angular, often intensely roughened, facet (see Fig. F7). Malarz (2005) reported that the proportion of broken and split clasts increased after flood events in two streams in the Carpathian mountains by >14% at all sample sites and as much as 49% at one site.

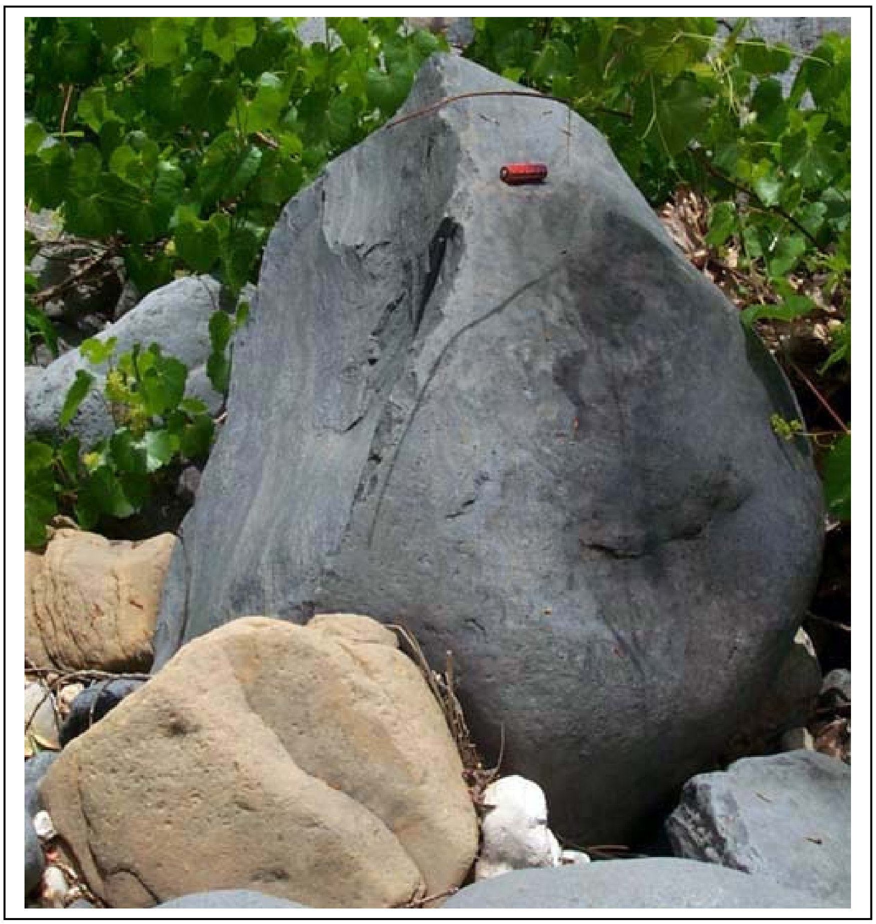

Figure F7 Flood transported basalt boulder in Oak Creek Canyon, Arizona. Boulder has been split from larger boulder (not in image) along angular facet on left. Note also the percussion pits on the surface of the sandstone boulder in the foreground. Image courtesy of M. Bourke.

<u>Percussion fracture facets</u> (concave and convex)

Scale: facet

Feature description:
During fluvial transport, clasts may collide with sufficient force to propagate percussion fractures (Fig. F2). Clast breakage by percussion, particularly on fine-grained rocks, creates smooth, shell-like convexities and concavities. These curvilinear facets may have secondary morphologies on their surface (*e.g.,* radial fissures, undulation marks) and these are described as sub-features following percussion fracture facets. Curvilinear facets were commonly observed on the basalt boulders at the Oak Creek Canyon field site in Arizona.

The size, angularity, and shape of a clast surface will affect the morphology of percussion fractures and their sub-features. It is generally thought that the angle at which two adjacent facets meet controls the fracture type. For example platform angles less than 90° are more conducive to the propagation of percussion fractures. Obtuse angles deter percussion fractures except in optimal situations in which exceptionally brittle, elastic stone is percussed with a relatively large amount of force.

The superposition and patina of percussion fracture faces may also provide useful evidence for the relative sequence of percussion events. Facets that crosscut fracture ridges are the result of subsequent percussion events. In addition, conchoidal fracturing exposes fresh, un-oxidized surfaces. If there is a measurable difference in the degree of patination between two percussion fracture facets, it is reasonable to infer separate events.

Figure F8 Flood-transported boulder, Oak Creek Canyon, Arizona. Note the presence of curvilinear (concave) facets. Image courtesy of M. Bourke.

Percussion fracture facet (cont.)

Figure F9 a & b Flood transported boulders from Oak Creek Canyon, Arizona. Note the preferential location of percussion fractures along the edge of the boulders. Image courtesy of M. Bourke.

Incipient cone

Scale: cm

Feature description:
Crescent or circular-shaped fractures form surface depressions as a result of clast impact. They often occur as rings that are 5-10 cm in diameter. In fluvial settings, the rounded geometry of clasts combined with relatively low-velocity collisions that often occur during transport, prevent percussion fractures from fully propagating. In these situations, a surface of relatively shallow crescent-shaped depressions is formed. These features are surface manifestations of subsurface hertzian cones (see below), hence they are termed incipient cones. In the fluvial literature, a second hypothesis for the presence of incipient cones is that they are caused by cavitation (see fig. 141a and b in Richardson and Carling, 2005). However, erosion of rock by cavitation in natural bedrock settings is not thought to be significant, as the natural roughness of the channel may substantially aerate the flow and inhibit cavitation (Hancock *et al.*, 1998).

Incipient cones are persistent features on rock surfaces, as they are zones of weakness and therefore locations of enhanced weathering (chemical and physical). As a result, their surface patterns become emphasized with time. In addition, as the fractures extend in a cone shape into the rock (mm to cm), the weathering can continue at depth.

Figure F10 Incipient cones on (from top to bottom) obsidian from Partridge Creek, Arizona, rhyolite from Partridge Creek, Arizona, quartzite from Cunene River N. Namibia, and quartzite from Finke Gorge, Australia. The crescentic depressions on the rock surfaces are the result of rock-to-rock collisions during flood events. Image collage courtesy of R. Haas.

Hertzian cone

Scale: mm to cm

Feature description:
Hertzian cones may be formed when the impact force is particularly high (Whittaker, 1994). In some rare instances, the full expression of a hertzian cone may be exposed on the surface of a clast, but more often only a portion of the cone is exposed (see Fig. F11). Typically, the hertzian cone remains in the subsurface (see incipient cones). Hertzian cones are also reported in the aeolian literature to describe abrasion marks at the micron scale from sand grain-to-grain impact (Greeley and Iversen, 1985; Marshall, 1979).

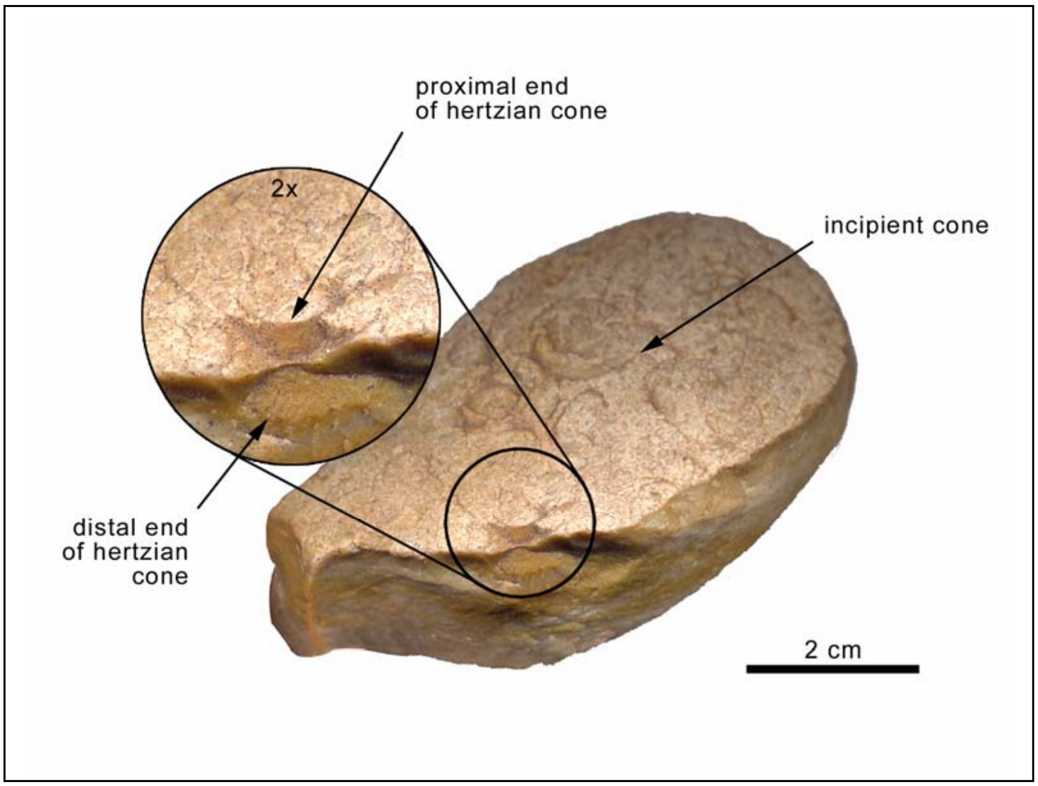

Figure F11 Partial hertzian cone exposed on the edge of a quartzite cobble from Finke River Gorge in central Australia. Note how the proximal end of the cone articulates with a circular depression on the surface. Image produced by R. Haas.

Percussion fracture ridge

Scale: facet

Feature description:
Percussion fractures are framed by ridges that define the extent of the fracture. These ridges are formed where a conchoidal facet intersects the original clast surface or another facet. In general, the angularity of the ridge, which can range from sharp to muted, is inversely related to the age of the percussion event as they are relatively susceptible to rounding. Facet ridges also influence the shape and path of subsequent percussion fractures as later impact fractures preferentially follow existing ridges. If there are no ridges to guide the force of percussion, then the percussion fractures will tend to fan out rapidly (Fig. F9). There are two general types of percussion fracture ridges: proximal and distal.

Proximal ridges result from the initiation of the percussion event. They are oriented roughly 90° to the percussion axis. The profile view of a proximal ridge is always acute for the core and obtuse for the flake (Cotterell and Kamminga, 1987). As a result, the proximal ridges often create surfaces amenable to subsequent percussion events (see Figs. F13 and F15).

Distal ridges are created where the force of percussion terminates. A series of distal ridges on the surface of a clast indicate multiple, often overlapping, percussion facets. Distal ridges on flakes almost always create angles of less than 90°, whereas those on cores are almost always greater than 90°. The importance of this is that sharper angled ridges on flakes have a tendency to round more quickly in fluvial environments and may explain the relative paucity of flakes in these environments.

Figure F12 Percussion fracture ridges (distal) (a) on a basalt clast in Oak Creek Canyon, Arizona. Muted ridge fractures are indicated (b). Image courtesy of M. Bourke.

Bulb of Percussion

Scale: sub-facet

Feature description:
A single bulb of percussion is almost always evident in a conchoidal fracture facet. On the proximal end of the concave facet of a core, the bulb of percussion describes a prominent dish-shaped surface (Fig. F13). The bulb represents a partial hertzian cone, which is responsible for initiating the conchoidal fracture. This feature always begins at the point of initiation and fans outward toward the distal end. Often the bulb of percussion terminates partway down the conchoidal fracture face, as in figure F15, but sometimes the bulb comprises the entire conchoidal fracture face (Fig. F13). For every concave bulb of percussion on a core, there is (or was) a conjugate flake with a convex bulb of percussion.

Figure F13 Overprinting of percussion fractures. a) Large step termination. b) Bulb of percussion. c) Radial fissures. Multiple smaller percussion marks overlap along the lower edge of boulder. Image courtesy of C. Matter.

Terminations

Scale: sub-facet

Feature description:
The morphology of a distal ridge varies according to the type of percussion termination. The interplay of many factors including impact geometry and force, surface morphology, and mineralogy affects the way a conchoidal facet terminates. There are three general types of percussion terminations (Cotterell and Kamminga, 1987): straight, outcurved or incurved (see Fig. F3). Outcurved terminations curve away from the mass of the clast and can be one of two types, hinge or step.

Hinge terminations are curvilinear and occur when the force of percussion abruptly but smoothly curves away from the mass of the core.

Step terminations are angular and occur when the flake breaks at a right angle to the facet plane. Step terminations typically occur when there is insufficient force to propagate a flake or where relatively low-angle, fragile rock surfaces have insufficient mass to bear the load of the percussion event. The latter situation is common on proximal ridges (Fig. F13).

Hinge and step terminations create topographic irregularities that deter subsequent percussion fractures from fully propagating. The result is that step fractures can "pile up" behind the initial step fracture. The accumulation is called *stacking* (see Fig. F15). Terminations are not mutually exclusive, as the length of a single distal ridge may include multiple termination types. The lateral margin of a percussion facet always has at least some length of feather termination, but the ridge at the distal end of the flake may exhibit multiple terminations.

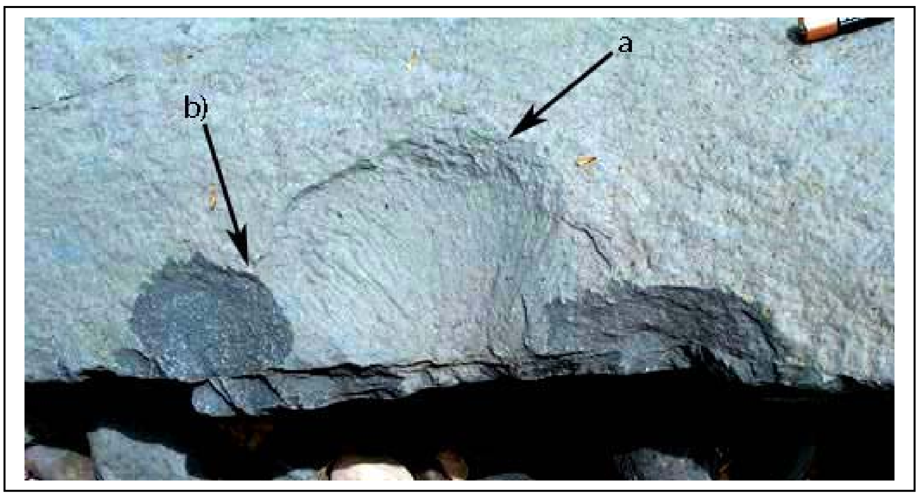

Figure F14 Feather termination (a) on basalt boulder, Oak Creek canyon, Arizona. Note that successive percussion events are evidenced by differential patina and overprinting (b) of the percussion fracture facets. Image courtesy of M. Bourke.

Terminations **(cont.)**

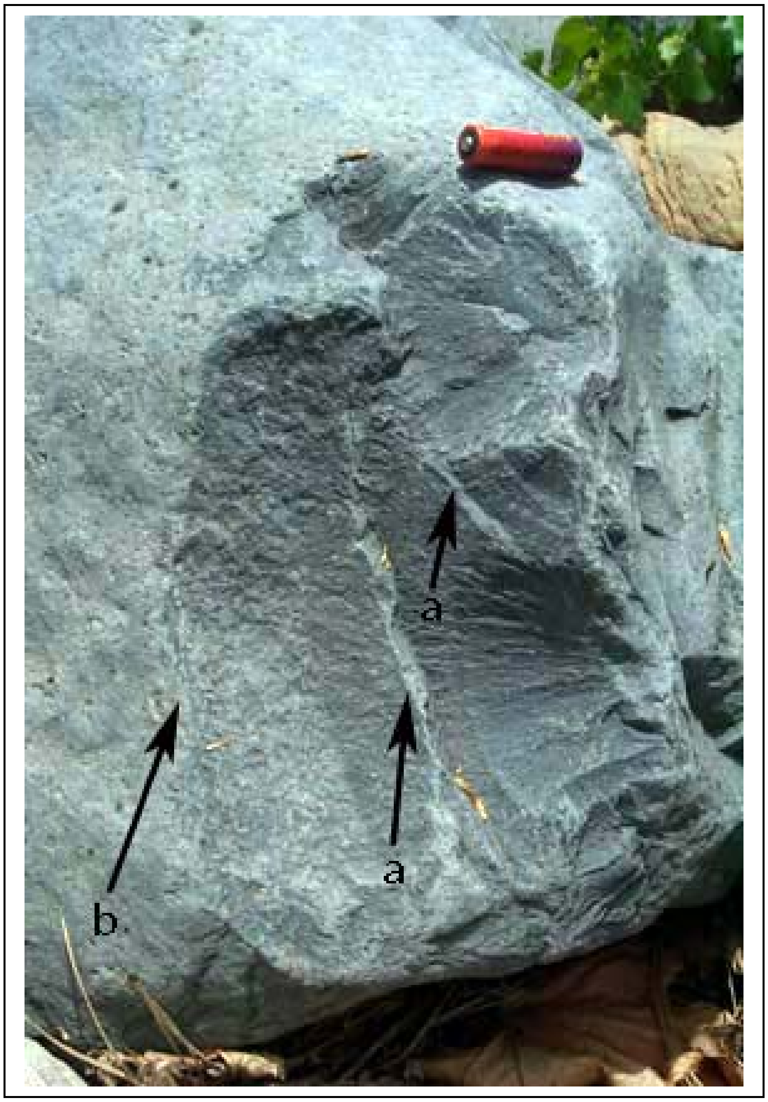

Figure F15 Step (a) and feather (b) terminations on basalt boulder, Oak Creek Canyon, Arizona. Note the *stacking* of percussion fractures and the radial fissures emanating from the point of impact. Image courtesy of M. Bourke.

Radial fissures

Scale: sub-facet

Feature description:
Radial fissures emanate from the point of impact in a radiating pattern and are the surface manifestation of a radiating shockwave. They tend to be topographically more prominent on relatively coarse-grained structures such as those in Figures F16 and F17.

Figure F16 Radial fissures on basalt boulder following percussion. Oak Creek Canyon, Arizona. See also Figures F13-15. Image courtesy of M. Bourke.

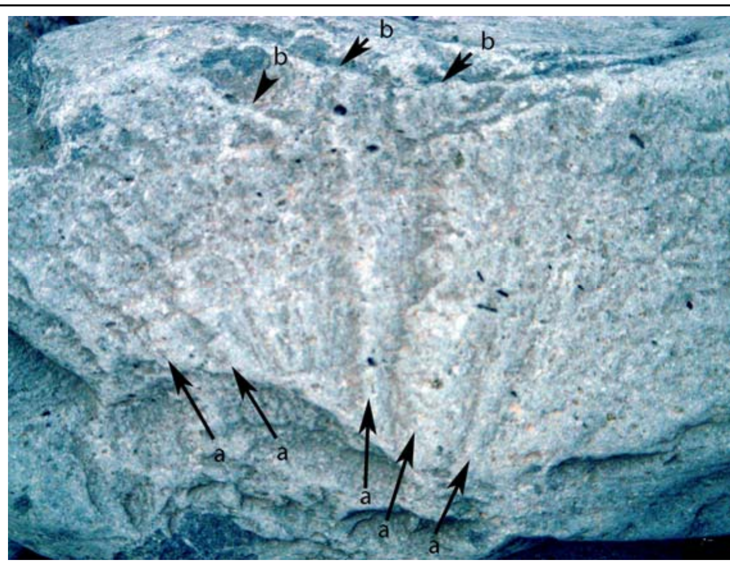

Figure F17 Large radial fissures (a) in Oak Creek Canyon, Arizona. Note modification and overprinting at edges by step terminations (b). Image courtesy of M. Bourke.

Undulations[1]

Scale: sub-facet

Feature description:
Undulations are concentric ridges that originate from the initiation point of a percussion fracture. They are aligned perpendicular to the direction of impact. Often, undulations have the greatest amplitude close to the impact point and frequency decreases with distance. However this needs to be tested with more field observations. Trends may be complex as multiple, embedded undulations can occur on the same facet.

Figure F18 Undulations on the surface of a fluvial boulder. The features display muting, likely by fluvial abrasion. Oak Creek Canyon, Arizona. Image courtesy of M. Bourke.

[1] These features are known as ripples in the archaeology literature, but the use of that term in this context is not appropriate given its existing use in fluvial and aeolian literature.

<u>Percussion pits</u>

Scale: clast

Feature description:
Percussion events often crush the mineralogical structure of the surface, resulting in pits (Figs. F7 and F19). These features occur in relatively non-brittle and/or heterogeneous materials. Some lithologies, *e.g.,* sandstone, will not usually propagate a percussion fracture. Instead, impacts tend to dislodge sand grains and leave a depression. However pits can co-occur with percussion fractures. Often, some degree of crushing may be evident at the initiation point of a percussion fracture. On stable clasts, the circular or ovoid planform may become modified by erosion focused on the downstream lip, and the percussion pits may become loci for incipient flute development (Richardson and Carling, 2005).

Figure F19 Flood transported clast in Oak Creek Canyon, Arizona showing percussion pits. Note step terminations at edge of percussion pits. Image courtesy of M. Bourke.

Striations/scratches

Scale: cm wide, mm deep

Feature description:
Rock striations, also known as tool marks, are formed on mobile clasts as they slide over protrusions (clasts and bedock) in the channel bed (Fig. F20). They also form on stationary clasts and bedrock by moving clasts. Striations are typically a few cm in length and commonly occur in groups which can be i) arranged simply, ii) aligned but not parallel or iii) in parallel, looped or arcuate pattern (Fig. F21) (see also Richardson and Carling, 2005). Occasionally they may form deeper rills (Bourke, 1990). Striations are also observed on rocks that have been glacially transported, but these can be distinguished from fluvial features by analysis of micro-features (*e.g.*, Van Hoesen and Orndorff, 2004).

Figure F20 Tool marks (rill-sized) on the under-side of the boulder (bright markings) indicates sliding and grinding movement of this 200 cm granite boulder over gravel, Cloghoge River, Co. Wicklow, Ireland. Both dark manganese staining and mm depth of granite were removed. Image courtesy of M. Bourke.

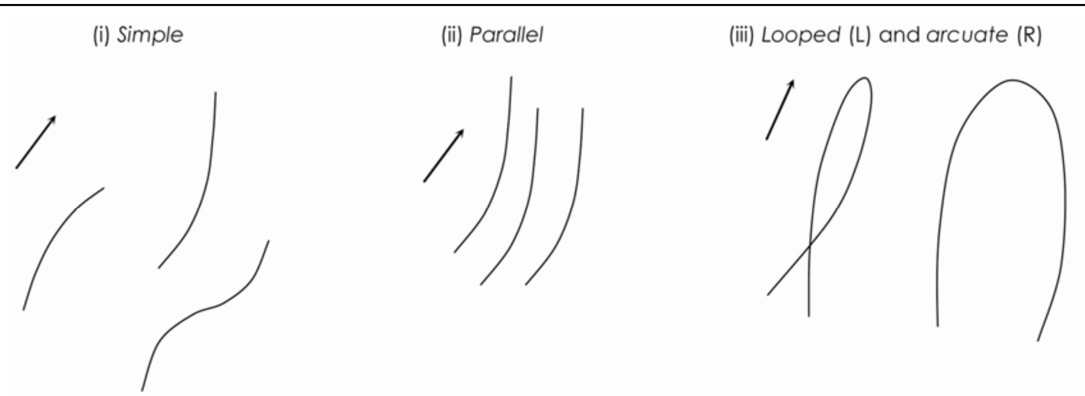

Figure F21 Schematic figure of striation patterns found in bedrock channels (after Richardson and Carling, 2005)

<u>Pothole</u>

Scale: cm to m

Feature description:
These are widely reported features in bedrock channels (*e.g.*, Baker and Pickup, 1987; Whipple *et al.*, 2000; Wohl, 1993; Wohl and Achyuthan, 2002). They are essentially circular (in plan view) deep depressions which are eroded by vortices (Richardson and Carling, 2005). They are common in constricted channel reaches and may take 10^3 yr to form in resistant rock (Wohl, 1998). They are often associated with joints, fractures and small channel bed irregularities (Hancock *et al.*, 1998). Potholes may evolve from the more rounded of the flute forms as erosion is focused downward rather than headward where vertical vortices act to selectively erode the flute bottom (Hancock *et al.*, 1998). Although potholes are not likely to form on transported clasts, they may enter the channel bedload system by erosion (undercutting, plucking) of bedrock.

Figure F22 a & b Segment of breached potholes formed in bedrock but subsequently entrained in the Cunene River, N. Namibia. Image courtesy of M. Bourke.

Figure F23 Pothole developed on megaclast in the Cunene River, N. Namibia. Image courtesy of M. Bourke.

Flutes

Scale: cm

Feature description:
Flutes form on megaclasts and bedrock from abrasion by suspended load (Baker and Pickup, 1987; Gupta *et al.*, 1999; Hancock *et al.*, 1998; Whipple *et al.*, 2000). In bedrock channels they are often well developed on the top of bedrock protrusions and the crest of large boulders. They are very well developed on fine grained rock and are associated with joints, fractures and small bed irregularities. Similar to their aeolian counterpart (see Figs. A7-A11), fluvial flutes are closed at the upstream end. They are thought to migrate in an upstream direction and occasionally have a more rounded rather than elongated shape. Hancock *et al* (1998) attributed this to a diminished strength of flow separation due to changes in the feature itself or in the surrounding bed. Flutes are poorly described in the fluvial literature and a comparative analysis with aeolian features is yet to be undertaken.

Figure F24 Spindle-shaped flutes (Richardson and Carling, 2005) developing at the sites of vesicles in volcanic rock (Rhyolitic agglomerate), Huai Nang Rong, Thailand. Flow from left to right. Image courtesy of K. Richardson.

Flutes (cont.)

Figure F25 *En echelon* flutes (Richardson and Carling, 2005) developed on Granitic gneiss megaclast, Nam Mae Chaem (Ob Luang), Thailand. Flow from bottom right to top left. The boulder is approximately 4 m across. Image courtesy of K. Richardson.

Figure F26 Large flute on megaclasts, Cunene River, N. Namibia. Image courtesy of M. Bourke.

Summary table of fluvial features

Clast Mobility	Scale	Feature
Transported & Non-transported	Clast	Round
		Polished & smooth
		fissure
		Broken and split clast
Transported & Non-transported	Facet	Percussion fracture facet
		Incipient cone
		Hertzian cone
		Percussion fracture ridge
		Bulb of percussion
		Termination
		Radial fissure
		Undulation
		Percussion pit
		Striation, scratches
Non-transported	Facet	Pothole
		Flute

Chapter 4: Weathering Features

Viles, H.A. and Bourke, M.C.

Alveoli on top of a weathered volcanic boulder in the Atacama Desert, Chile. Note large tafoni at base. Image courtesy of H. Viles.

Introduction

Mechanical, chemical and biological weathering processes all leave a range of clear morphological signatures on boulder surfaces. On Earth, weathering features produced in arid (hot and cold) and urban environments have been particularly well observed and categorized, and the major features identified from such extreme terrestrial environments are probably the most useful analogues for geomorphological interpretation on other planets. Often, combinations of weathering processes appear to act together or in sequence, to produce the observed breakdown features. This breakdown takes place predominantly *in situ* and movement of weathered materials is local and confined largely to the rock location. Even the unconsolidated rock residue may continue to break down in place until an end product, essentially in equilibrium with the environment, is formed. Many of the features assumed to be produced by weathering also have, perhaps superficial, visual similarities to those produced by aeolian processes.

Mechanical weathering involves the breakdown of rock material into smaller pieces without any change in the chemistry or mineralogy of the rock. Disintegration of rock material is achieved by the generation of forces within the rock mass. These forces are derived either from the growth of materials in voids (predominantly by frost action or the growth of salt crystals and occasionally by organic growths) or the internal expansion of rocks and minerals. The physical weathering processes associated with internal expansion include thermal expansion, unloading, hydration, wetting and drying, organic expansion and salt weathering (Dixon, 2004).

Chemical weathering processes are those which involve the chemical and or mineralogical transformation of rocks and minerals into products that are more in equilibrium with surface conditions. Several principal chemical weathering processes are recognized including solution (dissolution), hydrolysis, hydration, carbonation, chelation and redox reactions (oxidation and reduction) (Dixon, 2004).

Biological weathering by plants, lichens, algae and bacteria represents a significant contribution to the chemical weathering of rocks and minerals, primarily due to the fact that it produces abundant quantities of organic acids. On Earth most rock surfaces have some covering of micro-organisms in the form of a biofilm; although these do not always contribute to rock breakdown and may in fact form a bioprotective layer preventing other weathering agents from reacting with the rock (Carter and Viles, 2005).

In most environmental settings weathering processes act in combination and often synergistically. For example, physical weathering produces cracks and flakes, causing an increase in reactive surface area available for chemical weathering.

See Dorn and Cherveny (2005) for other useful images of weathering features.

Rounded clast

Scale: clast

Feature description:
Rounded clasts can be produced by intense weathering. Chemical weathering within soils and deep weathering mantles in humid tropical areas has often been seen to produce rounded 'corestones' of 'spheroidal weathering' on rocks such as granite. However, such rounded blocks can also be produced within shallow soils and saprolites as recorded in southern Sweden (Lidmar-Bergstrom *et al.*, 1997), the Sudetes, and Nova Scotia (Migon, 1999). Exfoliations caused by salt weathering and other processes within arid areas can also produce rounded rocks (as shown in Fig. W1). Lithological control (including fracture density and pattern) is probably important – some rock types (*e.g.,* granitoid and basaltic rocks) are more likely to produce rounded residual boulders than others. Rounded clasts can also be produced by a range of other rock breakdown processes including abrasion during fluvial transport.

Figure W1 Extreme spalling and flaking of a rounded granite clast in the central Namib Desert. Image courtesy of H. Viles.

Angular clast

Scale: clast

Feature description:
Weathering by freeze-thaw action in periglacial areas is often assumed to produce angular clasts as is weathering in hot deserts (Cooke *et al.*, 1993). Physical weathering processes, such as freeze-thaw and salt weathering often cause flaking and spalling of the surface which can create angular residual clasts. Lithological control is probably critical to the exact shape produced from such processes with fracture density and pattern an important control, and not all clasts weathered by freeze-thaw are angular (*e.g.*, Hall and Hall, 1991). Furthermore, as a very wide range of breakdown processes may produce angular clasts it is a difficult clast property to use confidently as diagnostic of any particular process regime.

Figure W2 Angular basalt clasts affected by mechanical weathering, near Purros, N Namibia. Image courtesy of H. Viles.

Split rock

Scale: clast

Feature description:
Intense physical weathering can enhance pre-existing weaknesses (such as fractures or joints) within boulders and produce split rocks (called Kernsprunge in German). Within deserts, many 19th century explorers reported hearing 'pistol shots' at night and finding split rocks the next morning, suggesting that dramatic cracking may occur under intense heating and cooling regimes. Lightning and fire have also been reported to produce split rocks (Dorn, 2003). Under experimental conditions such processes have been hard to reproduce, and moisture may be necessary to encourage splitting. Ollier (1971) also notes that split rocks can be produced by unloading affecting corestones within a weathered rock layer. The processes responsible for split rocks may be scale-dependent: larger split blocks may be produced by unloading, whereas smaller split blocks are likely to be formed by physical weathering. However, boulder to boulder collisions or impacts may also cause split rocks, so care needs to be taken in diagnosing the setting of the split rock before a confident identification of the formative process regime can be made.

Figure W3 Split rock from the Atacama Desert, Chile. Volcanic rocks in the coastal plain here are affected by intense heating and cooling as well as salt weathering. Image courtesy of H. Viles.

Pedestal/undercut rock

Scale: clast

Feature description:
In several rock types weathering may become concentrated at the base of boulders, producing undercutting and the development of small pedestals. They are also referred to as mushroom rocks, flared rocks, balanced rocks and perched blocks although there is some terminological confusion between boulders with true pedestals and those that are simply resting on a surface (Twidale, 2004). Undercut rocks are particularly well developed in sandstone, limestone and granite. The causes for such features are hotly debated, with some workers ascribing them to enhanced weathering below a cover of soil or sediment which has subsequently been removed. Others, however, implicate aeolian processes or shadow weathering (Schattenverwitterung) in producing the undercut elements, without any need for a former soil or sediment covering. Twidale (2004) provides a good review of the debate. It is most probable that several different process combinations could produce such features.

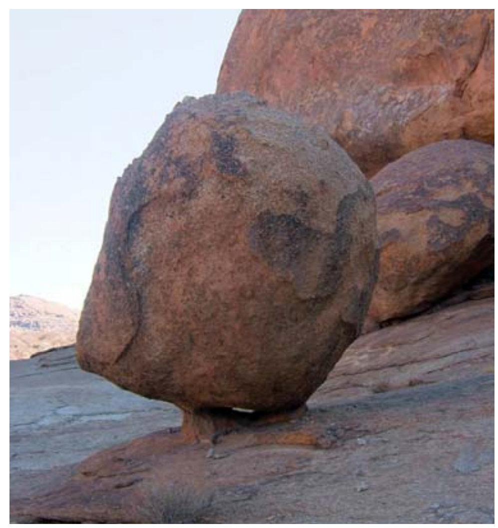

Figure W4 Pedestal rock in granite from Ameib Ranch, Namibia. Image courtesy of H.Viles.

Figure W5 Pedestal rock in sandstone Finke River Gorge, central Australia. Image courtesy of M. Bourke.

Doughnut rock

Scale: clast

Feature description:
Rounded boulders can become hollowed out in the middle to produce an annular-shaped clast. The processes responsible have not been described (as far as we are aware), and the only observations we can find of such features are from the Atacama Desert, Chile and Antarctica. Such features should not be confused with the 'rock doughnuts' observed on some granite outcrops, which are pits surrounded by a raised rim (Campbell, 1997). Morris *et al.,* (1972) described 'potholes' in sandstone in the dry valleys in Antarctica. They suggest that the holes are enlarged by freeze-thaw action of snow melt that has collected in a hollow. They do not speculate on how they are initiated. Perhaps the features in Figures W 6 and W7 are examples of breached 'potholes'. Similar pot hole morphologies are formed by fluvial processes (see Fig. F22 & F23).

Figure W6 Doughnut rocks formed by weathering of volcanic rocks in the Atacama Desert, Chile. Image courtesy of H. Viles.

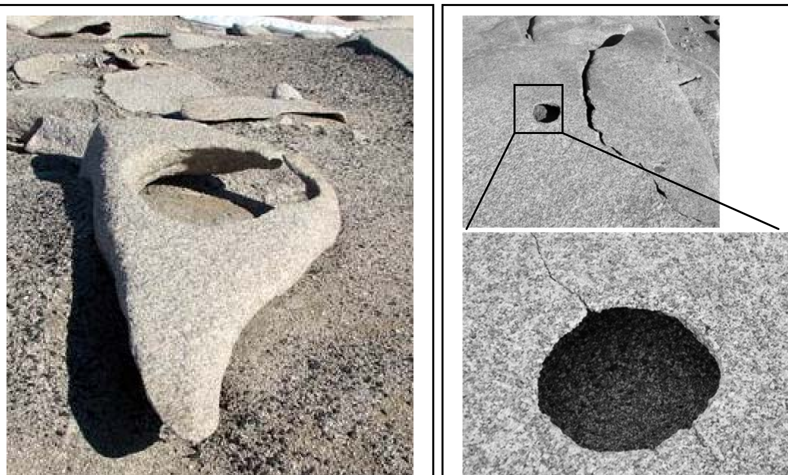

Figure W7 a and b Doughnut rocks (left) and pothole (right) near Lake Vida, Dry Valleys, Antarctica. Image courtesy of M. Badescu and S. Sherrit.

Microsolutional features

Scale: mm to cm

Feature description:
Small, often dendritic and curvilinear rills or grooves are found on rock surfaces. Their occurrence is restricted to soluble rocks within arid environments. They were first described by Lowdermilk and Woodruff (1932) who named them 'rillensteine'. It is hypothesized that these features are produced through chemical weathering where water availability is low, thus only small features result. Often they are found on ventifacts. It has been suggested that wind-driven films might, on occasion, produce rillensteine with preferential orientations to prevailing winds (*e.g.*, Maxson, 1940). A whole suite of similar features can be observed which are miniature versions of the karren features found on soluble rocks under humid conditions. (see Fig. 21.4 in Cooke *et al.*, 1993).

Figure W8 Microsolutional features formed on a basalt clast from NW Namibia. Image courtesy of H. Viles.

Figure W9 a & b Microsolutional features formed on ventifacts from California. Images courtesy of J. Fonseca.

Weathering grooves/rills

Scale: cm

Feature description:
Most grooves or rills produced by weathering are part of the suite of karren features developed as a result of solution of soluble rocks. They are most commonly noted on carbonate rocks, but can, in fact, develop on any soluble rocks such as gypsum and halite. They are usually found on steeply dipping surfaces and consist of a collection of parallel grooves, with U shaped cross-profiles. Each groove is separated from its neighbor by a sharp edge. They start at the crest of a slope or facet and die out downslope. Widths are characteristically 1 – 3 cm and length is some 10s of cm. Sweeting and Lancaster (1982) discuss their occurrence alongside aeolian grooves and flutes on carbonate rocks in the central Namib Desert. Similar grooves produced by weathering are also found on granitoid rocks and sandstones, although in this case solutional processes are probably not the dominant formative agent (Migon, 2006; Twidale, 1982). Many of the grooves on sandstones and granitic rocks are much larger than rillenkarren found on limestone.

Figure W10 Rillenkarren on massive limestone, Napier Range, NW Australia. Image courtesy of A.S. Goudie.

Micropitting

Scale: mm – cm

Feature description:
On many different rock types small pits can be produced by chemical and biological weathering, often developing from microscale irregularities within the rock surface which may be lithologically controlled (*e.g.*, vesicles in basalt). Lichen fruiting bodies, for example, are known to form small circular depressions in limestones (Danin and Garty, 1983).

Figure W11 Micropitting formed in fine-grained basalt, McMurdo, Antarctica. Image courtesy of G. Osinski.

Figure W12 Micropitting formed in dolerite, Transantarctic Mountains, Antarctica. Image courtesy of G. Osinski.

Weathering pits

Scale: cm to m

Feature description:
A whole range of names have been applied to pits produced by weathering (*e.g.*, gnamma, opferkessel, pias, vasques) which can occur over a wide range of scales and are found on many different rock types. On soluble rocks, such as limestone, such features are often ascribed to dissolution, and are found in association with other karren features, and given names such as kamenitza. Weathering pits have also been extensively recorded on granite and similar rocks, ranging in diameter from 15-20 cm to a few meters (Migoń, 2006). Large weathering pits may have overhanging or flared sidewalls. There is still much discussion on how pits develop in rocks that produce insoluble weathering residue.

Figure W13 a & b. Kamenitza (white arrows) and rillenkarren (red arrow) on limestone in the southern Namib Desert. Image courtesy of H. Viles.

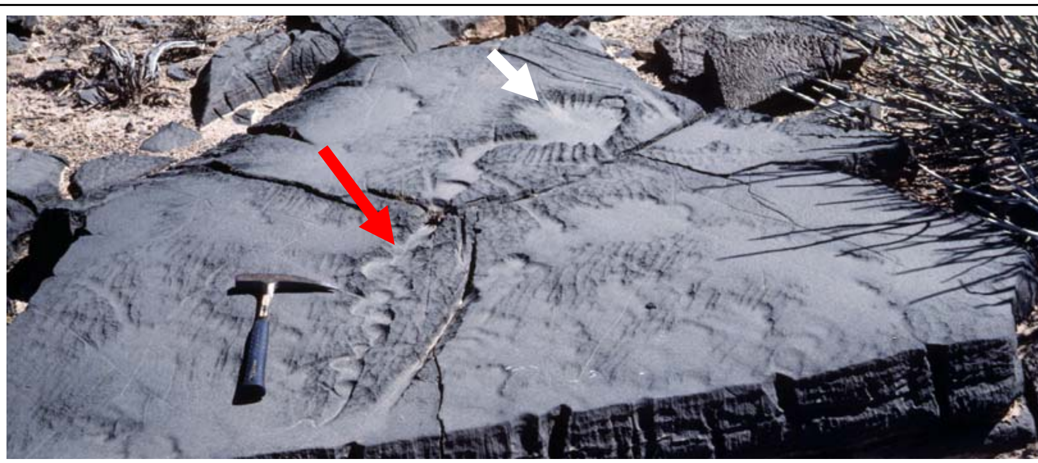

Granular disintegration

Scale: mm to cm

Feature description:
Granular disintegration is, strictly speaking, a type of breakdown process whereby weathering of various sorts (solution of soluble cement, stress induced by volumetric expansion, release of residual stress, water adsorption (Nicholson, 2004)) acts to detach individual grains from a rock surface, usually producing a roughened surface. The product is often loose, coarse grained debris which can easily be removed by erosional agents such as wind, water or gravity. This form of rock breakdown occurs commonly in coarse grained rocks such as sandstone, dolerite and granite. Clay-rich sandstones are thought to be particularly susceptible (Smith *et al.*, 1994). Granular disintegration produces a very similar effect to differential weathering in poly-mineral rocks, whereby particularly susceptible minerals are preferentially weathered out creating a pitted or roughened surface. Sparks (1971), shows an example where rhomb-shaped phenocrysts of feldspar have been weathered out from a boulder in Norway leaving a roughened surface.

Figure W14 Roughened surfaces caused by differential weathering of minerals within coarse granitoid rock, NW Namibia. Image courtesy of H. Viles.

<u>Alveoli or honeycombs</u>

Scale: cm

Feature description:
Alveoli are small (less than about 1m) cavernous weathering features which usually occur in groups. Individual alveoli are separated from their neighbors by narrow, intricate walls, creating an overall honeycombed surface. Many different weathering processes have been implicated in their formation, and they occur in a wide range of terrestrial environments (*e.g.,* coastal outcrops, Antarctica and hot deserts). Alveoli commonly form on large boulders and can cover whole facets. Their initiation and outline shape may be constrained by lithological variations, but they appear to develop by positive feedback in that once a hollow is initiated it creates an environment in which weathering is favored (Smith and McAlister, 1986).

Figure W15 Alveoli developed in mica schist, NW Namibia. The large heart-shaped hollow in the centre of the image is approximately 10 cm in diameter. Image courtesy of M. Bourke

Figure W16 Alveoli developed in sandstone, Fink River Gorge, central Australia. Note flaking on back wall. Image courtesy of M. Bourke

Tafoni

Scale: m.

Feature description:
Tafoni are large (usually over 1m in diameter) cavernous weathering features. Often developed towards the base of large boulders, they are characterized by having a flaking backwall (when actively forming), and an overhanging lip in front. The opening of the tafoni is often near-circular. They are a common feature of deserts, semi-arid regions and near coasts or anywhere salts can precipitate from dew or fog (Mustoe, 1982; Young, 1987). They occur in a wide range of lithologies but particularly in medium and coarse grained granites, sandstones and limestones. They are thought to be the result of flaking and granular disintegration (caused by hydration, salt crystalisation and chemical attack caused by saline solutions, Goudie, 2004a). Some tafoni have overhanging visors or rims that partly enclose the opening. In permeable sandstones, volcaniclastic rocks, and limestone, secondary cementation by precipitates in the outer layers may contribute to the resistant visors (Bloom, 1998; Martini, 1978). Tafoni have been recorded as developing over periods of around 10^4 yrs in Arizona, but very different rates of formation may occur in other areas (Norwick and Dexter, 2002).

Figure W17 Tafoni on large boulder, near Lake Vida, Dry Valleys, Antarctica.
Image courtesy of M. Badescu and S. Sherrit.

Figure W18 Well-developed and eroding tafoni in volcanic rock, showing spalling from the back wall. Atacama Desert, Chile. Image courtesy of H. Viles.

Basal hollow ('shark's fin' weathering)

Scale: cm

Feature description:
In many arid environments, especially where the surficial sediments are salt-rich, weathering is concentrated in the near-surface zone. Below the surface, and within a blanket of sediment, boulder surfaces are relatively pristine and unweathered. However, a highly aggressive weathering environment is found at the surface. This zone often produces accelerated weathering and the formation of a basal hollow.

Figure W19 Basal hollow above a basal sill on volcanic rock clast. Clast was removed from partial burial on a salty surface, Atacama Desert, Chile. Image courtesy of H. Viles.

Flaking

Scale: mm to cm

Feature description:
Flaking surfaces are produced where a range of weathering processes acts to remove sections of the near-surface layer. The lithological characteristics of the rock often determine the size and nature of the flakes removed, which can vary from tiny, thin mm to cm sized flakes. Layered and foliated rocks are particularly susceptible to flaking, as are those where surface crusts have developed. Migoń (2006) defines flakes on granite as being less than 1 cm thick.

Figure W20 Flaking on a small metamorphic rock clast from NW Namibia. Image courtesy of H. Viles.

Spalling

Scale: cm to m

Feature description:
Spalling is the peeling off of platy fragments from the surface of a rock. It is differentiated from flaking merely by being larger. Often parts of the surface of boulders, some 10s of cm in diameter and generally 1-5 cm in thickness, become detached by a combination of weathering processes. Migoń (2006) defines granite spalls as being between 1 and 30 cm thick, and up to 5 m^2 in surface area. Layered, foliated, crusted or case hardened rocks are particularly susceptible to spalling. Lithological controls, coupled with suitable penetration of water and temperature fluctuations, may determine whether rocks suffer flaking or spalling. Spalling may be accompanied by surface alteration or case hardening.

Figure W21 Spalling mica schist boulder from Cunene Sand Sea, NW Namibia. Note large detached fragment to left of rock. Image courtesy of H. Viles.

Multiple splits

Scale: cm

Feature description:
Instead of merely suffering from surface loss, as is the case for rocks affected by granular disintegration, flaking and spalling, some (especially small) clasts can break down as a result of the development of one, or more commonly a suite of, parallel fractures cutting through the whole rock (like a sliced loaf of bread). Such split rocks have been described in many deserts and differential receipt of solar radiation may be an important cause (McFadden *et al.*, 2005). Multiple splits have also been observed on high latitude coasts, ascribed to hydration (P. Migoń, *pers. comm.*).

Figure W22 Multiple splits forming in salt-affected limestone from UAE. Image courtesy of A.S. Goudie.

Cracks and polygonal cracking

Scale: mm – m

Feature description:
Cracks or fissures may form in clasts and boulders for a number of reasons (differential expansion with pressure release; thermal expansion and contraction; growth of foreign crystals in cracks and pores (Bloom, 1998)), but weathering and displacive growth of secondary minerals may be a particularly important cause of fissuring in arid areas. Where joints and linear planes of weakness exist in rocks, salt weathering and the growth of gypsum may cause these to become clearly fissured and forced apart. Ollier (1965) proposed a mechanism called 'dirt cracking' whereby dust blowing into cracks induced by thermal expansion and contraction reinforces the development of the cracks. Hall and Hall (1991) proposed that fracture patterns can reveal something about the formative processes responsible, drawing an analogy between the hierarchical crack patterns with 90^o angles between crack sets found on high altitude boulders with those produced in thermal shock experiments on ceramics. Sandstones, granites and more rarely basalts, andesites and limestones sometimes show distinctive patterning by networks of shallow cracks joining at around 120^o angles to produce polygons (Williams and Robinson, 1989). The cracks are often shallow (usually less than 1 cm) and the resultant polygons are usually around 10 cm in diameter. Polygonal cracking (also known as pachydermal weathering, elephant skin and tortoise shell, Thomas *et al.*, 2005) occurs commonly in hot dryland environments, but is also reported from the humid temperate zone. A number of hypotheses have been proposed to explain the development of polygonal cracking, such as thermal expansion and contraction, frost weathering or wetting and drying, but none satisfactorily explain all occurrences. Williams and Robinson (1989) propose that case hardening is an essential precursor to polygonal cracking.

Figure W24 Fissuring through displacive growth of gypsum in limestone, Namib Desert. Image courtesy of H. Viles.

Cracks (cont.)

Figure W24 a & b. Polygonal cracking on sandstone, Finke River Gorge, central Australia. Image courtesy of M. Bourke.

Case hardening

Scale: mm to cm thick, several cm^2

Feature description:
Many rock types, including sandstone, granite and limestone, are prone to hardening of the near-surface layer, thought to be caused by migration of pore fluids, which then evaporate and leave behind soluble minerals. These minerals increase cementation within this near-surface layer, causing a hardened skin to develop. Case hardening is often important in the development of subsequent weathering features, such as polygonal cracking. Micro-organisms have been seen to play a role in case hardening in some cases, but purely chemical processes may also be involved (Viles and Goudie, 2005).

Figure W25 Case hardening on quartzite cobble, Cunene River terrace, NW Namibia. Image courtesy of M. Bourke.

Calcite crusts

Scale: mm to cm

Feature description:
In areas where there is abundant calcium carbonate, precipitation on the surfaces (especially the undersides) of boulders can occur. The calcite crust is often complexly textured, with cauliflower–like growths common. Other minerals may also be precipitated in crusts, such as gypsum (dominantly in arid environments), calcium nitrate (sometimes called caliche and found in hyper-arid environments) or silica (sometimes found as silica speleothems in granite terrains). Under some circumstances such crusts can become displacive and cause cracking of the boulder.

Figure W26 Calcite precipitating around the margins and underside of quartzite clast in NW Namibia. Image courtesy of Heather Viles.

Rock varnish

Scale: microns thick, mm to cm^2 surface area coverage

Feature description:
Rock varnish is a coating found on many rocks in arid environments, enriched in manganese and iron, which usually imparts a red or black colouration to the underlying rock, depending on the detailed chemistry. It is also commonly observed to have a shiny appearance, probably because of the presence of lustrous minerals and its smooth, lamellate surface microtexture (Dorn, 1998). Wind abrasion has been observed to breakdown rock varnish. On the other hand, rock varnish has also been noted to form over ventifact surfaces, implying a shift in process regimes. Although included in the weathering chapter, rock varnish is usually thought of as having a largely external source. Silica glazes have also been observed on many rock surfaces ranging in colour from translucent to reddish brown or black. Dorn (1998) provides a wide review of many different types of varnish and rock coatings.

Figure W27 Patchy rock varnish developing on quartzite clast, NW Namibia. Image courtesy of H. Viles. Coin for scale at bottom on image.

Salt efflorescence/salt tides

Scale: cm

Feature description:
In arid and hyper-arid environments, salts crystallize out of solution easily and may become deposited on rock surfaces. In the Atacama Desert, on a range of igneous rocks, two distinctive types of salt accretion have been observed. Firstly, clear cauliflower-like growths of salts have been found in alveoli. Secondly, salt 'tides' – near-horizontal lines of amorphous salt deposits near the base of boulders (or at the height to which capillary rise might reach) - have been recorded (Heslop, 2003). Gypsum is also known to form destructive 'whiskers' (J. Clarke, *pers. comm*.)

Figure W28 Thick efflorescence of salt around boulders of volcanic rock in the Atacama Desert, Chile near Iquique. Image courtesy of H. Viles.

Figure W29
Salt precipitated from sublimated snow, on dolerite, Transantarctic Mountains, Antarctica. Image courtesy of G. Osinski.

Dust coating

Scale: microns thick, cm to m^2 surface coverage

Feature description:
As with desert varnish, dust coatings are largely produced by external material adhering to the surface of a boulder (rather than a product of weathering). However, once formed, they may react with the underlying surface. Usually recorded as thin, light brown films on the surface, dust films have only been rarely recorded in the literature (Dorn, 1998). Dust is commonly entrained in winds in arid and semi-arid areas and the clay sized particles may easily become accreted on rocks.

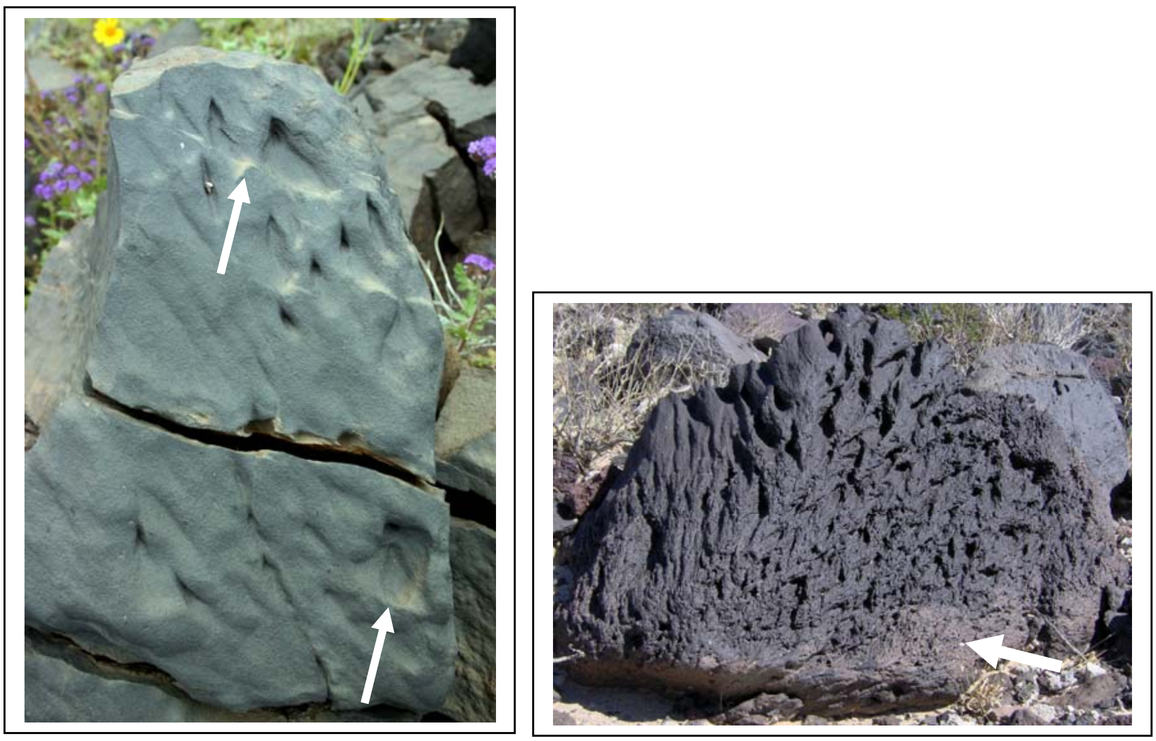

Figure W30 a & b Dust coatings in flutes (left) and at base of basalt boulders (right), Cady Mountains, California. Images courtesy of J. Laity.

Debris apron/grus

Scale: cm to m

Feature description:
Granular disintegration, flaking and other weathering processes produce particulate debris which, under some circumstances, builds up an apron around the weathering boulder. The term grus is often used to describe such a covering in which sand and gravel-sized material dominates (Migon, 2004).

Figure W31 a & b Debris apron adjacent to a large mica schist boulder near the Cunene River, NW Namibia. Image on right is close up of same apron. Image courtesy of M. Bourke.

Summary table of weathering features

SCALE	TYPE	NAME
CLAST		ROUNDED CLAST
		ANGULAR CLAST
		SPLIT ROCK
		PEDESTAL/UNDERCUT ROCK
		DOUGHNUT ROCK
FACET	MATERIAL LOSS	MICROSOLUTIONAL FEATURES
		WEATHERING GROOVES & RILLS
		MICROPITTING
		WEATHERING PITS
		GRANULAR DISINTEGRATION
		ALVEOLI
		TAFONI
		BASAL HOLLOW
		FLAKING
		SPALLING
	NO MATERIAL LOSS OR GAIN	MULTIPLE SPLITS
		CRACKS/POLYGONAL CRACKING
		CASE HARDENING
	MATERIAL GAIN	CALCITE CRUSTS
		ROCK VARNISH
		SALT EFFLORESCENCE/TIDES
		DUST COATING
		DEBRIS APRON/GRUS

NB, shaded cells are intermediate between material loss and no material loss or gain categories. Flaking, for example, ultimately results in material loss but the flakes can persist *in situ* for long periods

References

Allen, J. R. L. (1985). "Principles of Physical Sedimentology." George Allen & Unwin, London.

Andrefsky, W. (1994). Raw Material Availability and the Organisation of Technology. *American Antiquity* **59,** 21-35.

Baker, V. R., and Kale, V. S. (1998). The Role of Extreme Floods in Shaping Bedrock Channels. *In* "Rivers Over Rock: Fluvial Processes in Bedrock Channels." (K. J. Tinkler, and E. E. Wohl, Eds.), pp. 153-165. American Geophysical Union, Washington, DC.

Baker, V. R., and Pickup, G. (1987). Flood Geomorphology of the Katherine Gorge, Northern Territory, Australia. *Geological Society of America Bulletin* **98,** 635-646.

Beven, K. J. (1996). Equifinality and Uncertainty in Geomorphological Modelling. *In* "The Scientific Nature of Geomorphology." (B. L. Rhoads, and C. E. Thorn, Eds.), pp. 289-313. Wiley, Chichester.

Blair, T. C., and McPherson, J. G. (1999). Grain-Size and Textural Classification of Coarse Sedimentary Particles. *Journal of Sedimentary Research* **69,** 6-19.

Bloom, A. L. (1998). "Geomorphology: A systematic analysis of Cenozoic landforms." Prentice Hall, New Jersey.

Bosworth, T. O. (1910). Wind erosion on the coast of Mull. *Geological Magazine* **7,** 353-355.

Bourke, M. C. (1990). "The geomorphic effects of the August 1986 storm on a glaciated upland catchment in the Wicklow Mountains." Unpublished Masters thesis, University College Dublin.

Breed, C. S., McCauley, J. F., Whitney, M. I., *et al.* (1997). Wind erosion in drylands. *In* "Arid Zone Geomorphology: Process, Form and Change in Drylands." (D. S. G. Thomas, Ed.), pp. 437-464. Wiley & Sons, Chichester, New York, Weinheim, Brisbane, Singapore, Toronto.

Bridges, N. T., Greeley, R., Haldemann, A. F. C., *et al.* (1999). Ventifacts at the Pathfinder landing site. *Journal of Geophysical Research* **104,** 8595-8615.

Campbell, E. M. (1997). Granite landforms. *Journal of the Royal Society of Western Australia* **80,** 101-112.

Carter, N. E. A., and Viles, H., A. (2005). Bioprotection explored: the story of a little known earth surface process. *Geomorphology* **67,** 273-281.

Christiansen, H. H. (2004). Windpolished boulders and bedrock in the Scottish Highlands: Evidence and implications of Late Devensian wind activity. *Boreas* **33,** 82-94.

Cooke, R. U., Warren, A., and Goudie, A. S. (1993). "Desert Geomorphology." UCL Press Limited, London.

Cotterell, B., and Kamminga, J. (1987). The Formation of Flakes. *American Antiquity* **52,** 675-708.

Danin, A., and Garty, J. (1983). Distribution of cyanobacteria and lichens on hillsides of the Negev highlands and their impact on biogenic weathering. *Zeitschrift fur Geomorphologie* **27,** 413-421.

Dibble, H., and Whittaker, J. C. (1981). New Experimental Evidence on the Relation between Percussion Flaking and Flake Variation. *Journal of Archaeological Science* **8,** 283-296.
Dixon, J. C. (2004). Weathering. *In* "Encyclopedia of Geomorphology." (A. S. Goudie, Ed.), pp. 1108-1112. Routledge, London.
Dorn, R. I. (1998). "Rock coatings." Elsevier, Amsterdam.
Dorn, R. I. (2003). Boulder weathering and erosion associated with a wildfire, Sierra Ancha Mountains, Arizona. *Geomorphology* **55,** 155-171.
Dorn, R. I., and Cherveny, N. V. (2005). Atlas of Petroglyph Weathering Forms used in the Rock Art Stability Index (RASI). Available at http://alliance.la.asu.edu/rockart/stabilityindex/RASIAtlas.html.
Evans, J. W. (1911). Dreikanter. *Geological Magazine* **8,** 334-345.
Frich, P. (1988). "An analysis of climatic and geomorphological conditions for the abrasion by wind-blown snow in west Greenland." Unpublished M.Sc. thesis, University of Copenhagen.
Golombek, M. P., Anderson, R. C., Barnes, J. R., *et al.* (1999). Overview of the Mars Pathfinder Mission: Launch through landing, surface operations, data sets, and science results. *Journal of Geophysical Research* **104,** 8523-8553.
Goudie, A. S. (2004a). Tafoni. *In* "Encyclopedia of Geomorphology." (A. S. Goudie, Ed.), pp. 1034-1035. Routledge, London.
Goudie, A. S. (2004b). Ventifact. *In* "Encyclopedia of Geomorphology." (A. Goudie, Ed.), pp. 1091. Routledge, London.
Greeley, R., and Iversen, J. D. (1985). "Wind as a geological process on Earth, Mars, Venus and Titan." Cambridge University Press, Cambridge.
Greeley, R., Squyres, S. W., Arvidson, R. E., *et al.* (2004). Wind-Related Processes Detected by the Spirit Rover at Gusev Crater, Mars. *Science* **305,** 810-813.
Gupta, A., Kale, V. S., and Rajaguru, S. N. (1999). The Narmada River, India, through space and time. *In* "Varieties of Fluvial Form." (A. J. Miller, and A. Gupta, Eds.), pp. 113-143. John Wiley & Sons, Chichester.
Hall, K., and Hall, A. (1991). Thermal gradients and rock weathering at low temperatures: Some simulation data. *Permafrost and Periglacial Processes* **2,** 103-112.
Hancock, G. S., Anderson, R. S., and Whipple, K. X. (1998). Beyond Power: Bedrock River Incision Process and Form. *In* "Rivers Over Rock: Fluvial Processes in Bedrock Channels." (K. J. Tinkler, and E. E. Wohl, Eds.), pp. 35-60. American Geophysical Union, Washington, DC.
Heslop, E. E. M. (2003). "Clast breakdown in the Atacama Desert, Chile: An integrated field and laboratory approach." Unpublished D.Phil. thesis, University of Oxford.
Howard, A. D. (1998). Long Profile Development of Bedrock Channels: Interaction of Weathering, Mass Wasting, Bed Erosion, and Sediment Transport. *In* "Rivers Over Rock: Fluvial Processes in Bedrock Channels." (K. J. Tinkler, and E. E. Wohl, Eds.), pp. 297-319. American Geophysical Union, Washington, DC.
King, L. C. (1936). Wind-faceted stones from Marlborough, New Zealand. *Journal of Geology* **44,** 201-213.
Knight, J. (2005). Controls on the formation of coastal ventifacts. *Geomorphology* **64,** 243-253.

Knight, J., and Burningham, H. (2001). Formation of bedrock-cut ventifacts and late Holocene coastal evolution, County Donegal, Ireland. *Journal of Geology* **109,** 647-660.

Knight, J., and Burningham, H. (2003). Recent ventifact development on the central Oregon coast, western USA. *Earth Surface Processes and Landforms* **28,** 87-98.

Kuenen, P. H. (1928). Experiments on the formation of wind-worn pebbles. *Leidsche Geologische Medellingen* **3,** 19-38.

Kuenen, P. H. (1956). Experimental abrasion of pebbles, 2. Rolling by currents. *Journal of Geology* **64,** 336-368.

Laity, J. (1995). Wind abrasion and ventifact formation in California. *In* "Desert Aeolian Processes." (V. Tchakerian, Ed.), pp. 295-321. Chapman & Hall, London.

Laity, J. E. (1994). Landforms of Aeolian erosion. *In* "Geomorphology of Desert Environments." (A. D. Abrahams, and A. J. Parsons, Eds.), pp. 506-535. Chapman and Hall, London.

Lancaster, N. (1984). Characteristics and occurrence of wind erosion features in the Namib Desert. *Earth Surface Processes and Landforms* **9,** 469-478.

Lidmar-Bergstrom, K., Olsson, S., and Olvmo, M. (1997). Palaeosurfaces and associated saprolites in southern Sweden. *In* "Palaeosurfaces: recognition, reconstruction and palaeoenvironmental interpretation." (M. Widdowson, Ed.), pp. 95-124. Geological Society of London Special Publication No. 120.

Lowdermilk, J. D., and Woodruff, A. O. (1932). Concerning rillensteine. *American Journal of Science* **23,** 135-154.

Malarz, R. (2005). Effects of flood abrasion of the Carpathian alluvial gravels. *Catena* **64,** 1-26.

Marshall, J. R. (1979). "Experimental abrasion of natural materials." Unpublished Ph.D. thesis, University College London.

Marshall, P. (1927). The wearing of gravels. *Transactions of the New Zealand Institute* **58,** 507-532.

Martini, I. P. (1978). Tafoni weathering, with examples from Tuscany, Italy. *Zeitschrift fur Geomorphologie* **22,** 44-67.

Maxson, J. H. (1940). Fluting and faceting of rock fragments. *Journal of Geology* **48,** 717-751.

McCauley, J. F., Breed, C. S., and Grolier, M. J. (1979). Yardangs. *In* "Geomorphology in arid regions." (D. O. Doehring, Ed.), pp. 233-269. Annual Geomorphology Symposium, Binghampton, NY. Allen & Unwin, Boston.

McFadden, L. D., Eppes, M. C., Gillespie, A. R., and Hallet, B. (2005). Physical weathering in arid landscapes due to diurnal variation in the direction of solar heating. *Geological Society of America Bulletin* **117,** 161-173.

Migon, P. (1999). Residual weathering mantles and their bearing on the long-term landscape evolution of the Sudetes, NE Bohemian Massif, Central Europe. *Zeitschrift fur Geomorphologie Supplement Band* **119,** 71-90.

Migon, P. (2004). Grus. *In* "Encyclopedia of Geomorphology." (A. S. Goudie, Ed.), pp. 501-503. Routledge, London.

Migon, P. (2006). "Granite landscapes of the world." Oxford University Press, Oxford.

Morris, E. C., Mutch, T. A., and Holt, H. E. (1972). Atlas of geological features in the Dry Valleys of South Victoria Land, Antarctica, pp. 156. US Geological Survey Interagency report:Astrogeology.
Mustoe, G. E. (1982). The origin of honeycomb weathering. *Geological Society of America Bulletin* **93,** 108-115.
Nicholson, D. T. (2004). Granular disintegration. *In* "Encyclopedia of Geomorphology." (A. S. Goudie, Ed.), pp. 493-494. Routeledge.
Norwick, S. A., and Dexter, L. R. (2002). Rates of development of tafoni in the Moenkopi and Kaibab formations in Meteor Crater and on the Colorado Plateau, northeastern Arizona. *Earth Surface Processes and Landforms* **27,** 11-26.
Ollier, C. D. (1965). Dirt cracking - a type of insolation weathering. *Australian Journal of Science* **27,** 236-237.
Ollier, C. D. (1971). Causes of spheroidal weathering. *Earth Science Reviews* **7,** 127-141.
Powers, W. E. (1936). The evidences of wind abrasion. *Journal of Geology* **44,** 214-219.
Richards, K. (1982). "Rivers: Form and Process in Alluvial Channels." Methuen, New York.
Richardson, K., and Carling, P. A. (2005). A typology of sculpted forms in open bedrock channels. *Geological Society of America, Special Papers***,** 108pp.
Ritter, D. F. (1975). Stratigraphic Implications of Coarse-Grained Gravel Deposited as Overbank Sediment, Southern Illinois. *Journal of Geology* **83,** 645-650.
Schlyter, P. (1994). Paleo-periglacial ventifact formation by suspended silt or snow - site studies in south Sweden. *Geografiska Annaler, Series A* **76 A,** 187-201.
Schlyter, P. (1995). Ventifacts as palaeo-wind indicators in southern Scandinavia. *Permafrost and Periglacial Processes* **6,** 207-219.
Sharp, R. P. (1949). Pleistocene ventifacts east of the Big Horn Mountains, Wyoming. *Journal of Geology* **57,** 175-195.
Smith, B. J., Magee, R. W., and Whalley, W. B. (1994). Breakdown patterns of quartz sandstone in a polluted urban environment, Belfast, Northern Ireland. *In* "Rock weathering and landform evolution." (D. A. Robinson, and R. B. G. Williams, Eds.), pp. 131-150. Wiley, Chichester.
Smith, B. J., and McAlister, J. (1986). Observations on the occurrence and origins of salt weathering phenomena near Lake Magadi, Southern Kenya. *Zeitschrift fur Geomorphologie* **30,** 445-460.
Sparks, B. (1971). "Rocks and Relief." Longman, London.
Speth, J. D. (1972). Mechanical basis of percussion flaking. *American Antiquity* **37,** 34-60.
Speth, J. D. (1974). Experimental investigation of hard-hammer percussion flaking: The effects of oblique impact. *Tebiwa* **17,** 7-36.
Speth, J. D. (1975). Miscellaneous studies in hard-hammer percussion flaking: The effects of oblique impact. *American Antiquity* **40,** 203-207.
Speth, J. D. (1981). The role of platform angle and core Size in hard-hammer percussion flaking. *Lithic Technology* **10,** 16-21.
Sweeting, M. M., and Lancaster, N. (1982). Solutional and wind erosion forms on limestone in the Central Namib Desert. *Zeitschrift fur Geomorphologie* **26,** 197-207.

Thomas, M., Clarke, J. D. A., and Pain, C. F. (2005). Weathering, erosion and landscape processes on Mars identified from recent rover imagery, and possible Earth analogues. *Australian Journal of Earth Sciences* **52,** 365-378.

Tinkler, K., and Wohl, E. (1998). A Primer on Bedrock Channels. *In* "Rivers Over Rock: Fluvial Processes in Bedrock Channels." (K. J. Tinkler, and E. E. Wohl, Eds.), pp. 1-18. American Geophysical Union, Washington, DC.

Twidale, R. (1982). "Granite Landforms." Elsevier, Amsterdam.

Twidale, R. (2004). Pedestal rock. *In* "Encyclopedia of Geomorphology." (A. S. Goudie, Ed.), pp. 768. Routledge.

Van Hoesen, J. G., and Orndorff, R. L. (2004). A comparative SEM study on the micromorphology of glacial and nonglacial clasts with varying age and lithology. *Canadian Journal of Earth Sciences* **41,** 1123-1139.

Viles, H. A., Brearley, A. J., Bourke, M. C., and Holmlund, J. (2005). What Processes Have Shaped Basalt Boulders on Earth and Mars? Studies of Feature Persistence Using Facet Mapping and Fractal Analysis. *In* "LPSC XXXVI, abs. 2237."

Viles, H. A., and Goudie, A. S. (2005). Biofilms and case hardening on sandstones from Al-Quwayra, Jordan. *Earth Surface Processes & Landforms* **29,** 1473-1485 DOI: 10.1002/esp.1134.

Wentworth, C. K., and Dickey, R. I. (1935). Ventifact localities in the United States. *Journal of Geology* **43,** 97-104.

Whipple, K., Hancock, G., and Anderson, R. (2000). River incision into bedrock: Mechanics and relative efficiacy of plucking, abrasion, and cavitation. *Geological Society of America Bulletin* **112,** 490-503.

Whitney, M. I. (1979). Electron micrography of mineral surfaces subject to wind-blast erosion. *Geological Society of America Bulletin* **90,** 917-934.

Whittaker, J. C. (1994). " Flintknapping: Making and understanding stone tools." University of Texas Press, Austin.

Williams, R. B. G., and Robinson, D. A. (1989). Origin and distribution of polygonal cracking of rock surfaces. *Geografiska Annaler* **71,** 145-159.

Wohl, E. E. (1993). Bedrock channel incision along Piccaninny Creek, Australia. *Journal of Geology* **101,** 749-761.

Wohl, E. E. (1998). Bedrock Channel Morphology in Relation to Erosional Processes. *In* "Rivers Over Rock: Fluvial Processes in Bedrock Channels." (K. J. Tinkler, and E. E. Wohl, Eds.), pp. 133-152. American Geophysical Union, Washington, DC.

Wohl, E. E., and Achyuthan, H. (2002). Substrate influences on incised-channel morphology. *Journal of Geology* **110,** 115-120.

Wohl, E. E., and Ikeda, H. (1998). Patterns of Bedrock Channel Erosion on the Boso Peninsula, Japan. *The Journal of Geology* **106,** 331-345.

Young, A. R. M. (1987). Salt as an agent in the development of cavernous weathering. *Geology* **15,** 962-966.

About the Authors:

Dr. Mary Bourke is a Research Scientist at the Planetary Science Institute in Tucson and a Senior Research Associate at the University of Oxford. She is a geomorphologist who specializes in the fluvial and aeolian geomorphology of desert regions on Earth and on Mars.

Mr. J. Alexander Brearley undertook his undergraduate degree in Geography at Oxford and is currently undertaking a Ph.D in Oceanography at Southampton University.

Mr. Randall Haas is an archaeologist and GIS specialist with Western Mapping Company in Tucson, Arizona. His interests are in the use of stone tool analysis and geospatial methods to explore the social dynamics and behavioral ecology of hunter-gatherers and early agriculturists.

Dr. Heather Viles is Reader in Geomorphology at the University of Oxford. Her research focuses on rock breakdown and landscape evolution in a range of environments, as well as on the deterioration of building stones.

Heather Viles (left) and Mary Bourke (right) in the Cunene Sand Sea, Namibia.

ISBN 0-9785236-0-1